SAPIENZA
UNIVERSITÀ DI ROMA

DIPARTIMENTO DI BIOLOGIA E BIOTECNOLOGIE

"CHARLES DARWIN"

Ph.D. in

CELL AND DEVELOPMENTAL BIOLOGY

XXXV Cycle

(a.a. 2021-2022)

Molecular expression and characterisation of non-coding RNA in tumor growth and invasiveness of glioblastoma stem-like cells

Ph.D. Student

Chiara De Dominicis

Tutor

Rosa Sorrentino

Coordinator

Giulia De Lorenzo

Supervisor

Lucia Ricci Vitiani

INDEX

AIM OF THE WORK

The aim of my PhD project was the analysis of ncRNAs expression patterns in glioblastoma (GBM) and the characterisation of their role in tumor proliferation and invasiveness, using patient-derived glioblastoma stem-like cells (GSCs). GSCs are not only the most aggressive component of GBM, responsible for tumor initiation, progression, recurrence and therapeutic resistance, but also a powerful and innovative tool: they can be isolated from the tumor progenitor to generate self-renewing, multipotent and highly tumorigenic cell lines capable of mirroring the biology and functions of GBM better than any other cell lines, to the point that they could predict the response to therapy of the original tumor. For these reasons, studies that rely on GSCs as model may help to understand the complex biology of GBM and to unveil new biomarkers and/or new targets for innovative therapeutic approaches. Some novel targets could be found among the non-coding RNAs (ncRNAs), that are emerging from the "dark matter" of the genome as key regulators of physiological processes: in fact, ncRNAs have the potential to act as oncogenes and/or tumor suppressors, as well as, being involved in different mechanisms to regulate cancer states. Recent, accumulating evidence suggests that dysregulation of ncRNAs expression may affect glioma initiation and progression. Therefore, ncRNAs may represent biomarkers for glioma diagnosis, prognosis and target therapy and their study is an opportunity to design better therapeutic intervention for GBM. The lab directed by Dr Ricci-Vitiani is particularly interested in elucidating the role of ncRNAs in GBM using GSCs as *in vitro* and *in vivo* model, and they are focusing on the study of microRNAs (miRNAs) and long non-coding RNAs (lncRNAs).

They have recently analysed miRNA expression profiles in their collection of GSCs and have found that their expression from a large cluster (14q32) was significantly down-regulated compared to normal neural stem cells (NSCs). This cluster is located within a chromosomal region named DLK1-DIO3, that is known to be involved in differentiation and development, and a cancer-associated genomic region. Within the DLK1-DIO3 region, 54 miRNAs (cluster-14-miRNAs) are located and organised into sub-clusters 14A and 14B. These miRNAs are down-regulated in GBM, and their altered expression correlates with tumor aggressiveness and survival of GBM patients.

In accordance with these results, the aim of this study was to investigate the expression pattern and the role played by ncRNAs in GBM

pathogenesis, using patient derived GSCs as a model. My work began with the study of miR-370-3p, a miRNA belonging to DLK1-DIO3 domain and among the down-regulated ncRNAs in glioma tissues, particularly in recurrent GBM. Several studies reported that down-regulation of miR-370-3p is involved in tumorigenicity in other forms of cancer as well, while it may instead act as an oncosuppressor in glioma by inhibiting cell proliferation, when it is expressed. However, the full biological role and functional mechanisms of miR-370-3p are not fully known. To elucidate the oncosuppressing function of miR-370-3p in GBM, we restored its expression in GSCs via lentiviral transduction, using a TRIPZ doxycycline inducible vector. Subsequently, we analysed the impact of the miRNA restored expression on GSCs viability and malignant features, such as proliferation, invasiveness and clonogenic capability, *in vitro* and *in vivo*. We further investigated, by microarray, the complex interplay miR-370-3p is involved with, to identify partners and main mediators of its tumor suppressive function. After the gene expression analysis, we identified possible interaction partners of miR-370-3p and confirmed the predictions using a dual-luciferase reporter assay. We then used flow cytometry to identify possible indirect modulation by miR-370-3p towards other deregulated genes detected after gene expression analysis. We believe that exploring the role of miRNAs and their interactions with lncRNAs would deepen our understanding of GBMs and help unveiling novel diagnostic and therapeutic targets.

SUMMARY

Glioblastoma (GBM) is an aggressive form of glioma in adults that owes its worse characteristics, like recurrence and resistance to therapy, mainly to GBM stem-like cells (GSCs). *In vitro* studies employ GSCs to generate self-renewing cell lines that can mimic the original tumor. We performed analyses on our collection of patient-derived GSC lines to study long non-coding RNAs (lncRNAs) and micro RNAs (miRNAs), important oncogenic drivers and tumor suppressors in many tumors. Our work revealed that the microRNA miR-370-3p is significantly down-regulated in GSCs compared to a normal control and, when restored, the proliferation, migration and clonogenic abilities of GSCs are impaired. Another effect of miR-370-3p restoration became clear after gene expression analyses, which identified several transcripts involved in Epithelial to Mesenchymal Transition (EMT), and Hypoxia signalling pathways. Surprisingly, among the genes down-regulated as a result of miR-370-3p restored expression, we found more genes correlated to GBM, like the EMT-inducer high-mobility group AT-hook 2 (HMGA2), the master transcriptional regulator of the adaptive response to hypoxia, Hypoxia-inducible factor (HIF)1A, and the long non-coding RNA (lncRNA) Nuclear Enriched Abundant Transcript (NEAT1). In particular, NEAT1 is an oncogenic lncRNA, associated to worse prognosis for several cancers: we found by luciferase assay that miR-370-3p directly binds NEAT1, so that the expression levels of these ncRNAs are inversely correlated in GSCs. Our results suggest that a complex "cascade" interplaying among different ncRNAs is partially responsible for GBM's most malignant features. Indeed, miR-370-3p shows a prominent tumor-suppressor function by targeting mRNAs involved in EMT, in hypoxia pathways, and cell growth and the invasiveness enhancer NEAT1, making this microRNA another promising candidate for novel GBM treatments.

SOMMARIO

Il glioblastoma è una forma aggressiva di glioma negli adulti che deve le sue peggiori caratteristiche, quali la recidività e la resistenza alla terapia, principalmente alle GBM stem-like cells (GSCs). Studi *in vitro* usano le GSCs per generare linee cellulari auto-rinnovanti che possono mimare il tumore originale. Abbiamo analizzato la nostra collezione di GSCs derivate da pazienti, come strumento per studiare i long non-coding RNA (lncRNAs) e i micro RNA (miRNAs), importanti oncogeni e oncosoppressori in vari tipi di tumore. Il nostro lavoro ha rivelato che il micro RNA miR-370-3p è significativamente sottoespresso to nelle GSCs rispetto ai controlli, inoltre, il ripristino della sua espressione è in grado di ridurre le capacità di proliferazione, migrazione e clonogenicità delle GSCs. Una successiva analisi di espressione genica sulle GSCs ha identificato diversi trascritti coinvolti nelle vie di segnale correlate alla transizione epitelio/mesenchima (EMT) e all'ipossia. Sorprendentemente, tra i geni sottoespressi a seguito della espressione del miR-370-3p, abbiamo trovato più geni correlati al GBM, quali l'induttore dell'EMT, HMGA2 (high-mobility group AT-hook 2); il principale regolatore della risposta adattativa dell'ipossia, HIF1A; e il long non-coding RNA, NEAT1 (Nuclear Enriched Abundant Transcript). In particolare, NEAT1 è un lncRNA oncogenico associato ad una prognosi più sfavorevole in diversi tumori: abbiamo notato tramite saggio della luciferasi che il miR-370-3p interagisce direttamente con NEAT1, al punto che nelle GSCs le espressioni di questi ncRNAs sono inversamente correlate. I nostri risultati suggeriscono che un complesso gioco tra diversi ncRNAs sia parzialmente responsabile delle caratteristiche più maligne del GBM. In particolare, il miR-370-3p mostra un ruolo prominente di oncosoppressore bersagliando mRNAs coinvolti nelle vie di segnale dell'EMT, ipossia, e sull'enhancer di proliferazione e invasività NEAT1, rendendo questo microRNA un altro promettente candidato per nuove terapie contro il GBM.

SYNOPSIS

Gliomas are highly prevalent forms of brain tumor in humans and glioblastoma multiforme (GBM) is the most common and lethal form of glioma in adults (Tanaka, Louis et al. 2013) and is classified as a grade IV astrocytoma. GBM current gold standard treatment consists in a combination of surgical resection, radiation, and chemotherapy with temozolomide (TMZ). However, prognosis is alarmingly dismal, with a survival time of 14-15 months from the time of diagnosis, and only 5,8% of patients surviving up to 5 years post-diagnosis (Ostrom, Cote et al. 2018, Ostrom, Gittleman et al. 2018). Novel treatments have been proposed as additions to the gold standard, but identification of new drug targets has been unsuccessful, as targeted compounds that perform well in preclinical studies, fail *in vivo* (Szopa, Burley et al. 2017, Janjua, Rewatkar et al. 2021). Further studies have revealed how GBM's recurrence and resistance are induced, among other factors, by a subpopulation of cells, displaying stem-like properties reminiscent of normal stem cells, called GBM stem-like cells (GSCs) (Singh, Hawkins et al. 2004, Ahmed, Auffinger et al. 2013). GSCs can be isolated from the tumor to generate self-renewing, multipotent and highly tumorigenic cell lines (Gimple, Bhargava et al. 2019). These cells recapitulate the *in vivo* biology and functions of GBM, to the point that they can predict the response to therapy of the original tumor, attracting further studies on their physiology and processes (Lee, Kotliarova et al. 2006, Ernst, Hofmann et al. 2009, D'Alessandris, Biffoni et al. 2017, Gimple, Bhargava et al. 2019). It is known that a consistent portion of the untranslated genome is actually transcribed to produce non-coding RNAs (ncRNAs). ncRNAs are key regulators of physiological processes, also playing roles such as oncogenic drivers and tumor suppressors in many cancer types (Chan and Tay 2018, Slack and Chinnaiyan 2019). NcRNAs can be divided into classes, approximately based on their size (Esteller 2011). Currently, studies are focused on two main ncRNAs classes, micro RNAs (miRNAs) and long non-coding RNAs (lncRNAs), due to their ability to influence gene regulation across all cellular physiological pathways (Chi, Wang et al. 2019, Hill and Tran 2021, Woods and Van Vactor 2021). Analyses in GSCs have found that miRNAs expression is significantly down-regulated compared with normal neural stem cells (NSCs) (Aldaz, Sagardoy et al. 2013, Sana, Busek et al. 2018). These miRNAs originate mainly from a large cluster on chromosome 14 (14q32), located within a chromosomal region named DLK1-DIO3, that is known to be a cancer-associated genomic region (Benetatos, Hatzimichael et al. 2013). MiR-

370-3p is a miRNA belonging to DLK1-DIO3 domain. Several studies reported that down-regulation of miR-370-3p is involved in tumorigenicity in various forms of cancers, including glioma tissues and particularly, in recurrent GBM (Gao, Chen et al. 2016, Chen, Feng et al. 2018, Chen, Liu et al. 2019). Evidence suggest that this miRNA may act as oncosuppressor in glioma by inhibiting cell proliferation (Peng, Wu et al. 2016). The aim of this study was investigating the expression pattern and the role played by ncRNAs in GBM pathogenesis, using patient derived GSCs as a model. Analysing our collection of patient-derived GSCs and GBM tissues by Real-Time PCR (RT-PCR), we found that miR-370-3p was significantly down-regulated compared to normal brain tissues and (NSCs), respectively. Then, we restored miR-370-3p expression in GSC lines by using an inducible Tet-On lentiviral vector (TRIPZ) carrying pri-miR-370-3p in the 3'-untranslated region of Red Fluorescent Protein (RFP) to analyse the role of miR-370-3p on GSC tumorigenic properties. Ectopic expression of miR-370-3p significantly impaired GSCs viability, and the following assays showed a considerable inhibition of migration and colony formation capabilities. We then investigated the effects of miR-370-3p restoration in an orthotopic xenograft mouse model. After four weeks, the degree of brain invasion was significantly reduced in mice grafted with TRIPZ-miR-370-3p vector-transduced GSCs and no migration to the contralateral hemisphere was observed. The gene expression profiles of GSCs transduced with TRIPZ-miR-370 or TRIPZ empty vector were analysed by microarray and compared, looking for the most deregulated genes. We identified 81 genes assigned to pathways enriched with a p-value below 0.001. The results indicate that the most significantly enriched pathways were related to EMT and hypoxia. Among miR-370-3p potential target mRNAs, we found the high-mobility AT-hook 2 (HMGA2) group, which belongs to the high-mobility group (HMG) protein family and functions as an oncogene, and the Hypoxia-Inducible Factor (HIF) 1A. We found that the restoration of miR-370-3p induced a significant decrease of HMGA2 and HIF1A expression in both GSC lines analysed, indicating a direct targeting. To prove the direct targeting of HIF1A by miR-370-3p, we performed a dual-luciferase reporter assay and the results confirmed the predicted miR-370-3p - HIF1A interaction.

Interestingly, NT5E/CD73, an enzyme responsible for adenosine (ADO) production, was found among the most significantly down-regulated genes in miR-370 restored GSCs. When CD73 is down-regulated, cell

migration and invasion decrease in glioma, while the cytotoxic effect of TMZ is potentiated (Azambuja, Gelsleichter et al. 2019). MiR-370-3p does not directly target CD73, but there may be an indirect modulation through HIF1A, which binds to the NT5E promoter thereby activating CD73 expression (Synnestvedt, Furuta et al. 2002, Colgan, Eltzschig et al. 2006). Growing evidence have confirmed that miRNAs and lncRNAs can interact with each other in a sequence-specific manner (Ballantyne, McDonald et al. 2016). Through a dual-luciferase reporter assay we found a direct binding between miR-370-3p and the lncRNA Nuclear Enriched Abundant Transcript 1 (NEAT1), which is linked to hypoxia, promotes EMT, and correlates with higher World Health Organization (WHO) grade human glioma tissues (He, Jiang et al. 2016, Zhang, Wu et al. 2017, Kong, Zhao et al. 2019). As expected, miR-370-3p and NEAT1 expression levels are inversely correlated in both GBMs and GSCs, confirming that there may be a reciprocal regulation between miR-370-3p and NEAT1. Furthermore, we analysed the association of miR-370-3p and NEAT1 expression with survival of TCGA database patients: the expression level of miR-370-3p was not associated with prolonged value for survival in the analysed GBM patients, while high NEAT1 expression was associated to unfavourable overall survival. We then examined the effect of NEAT1 silencing by transducing lentiviral vector carrying short hairpin (sh)NEAT1 or shNTC (no target control) sequence and green fluorescent protein (GFP) as a reporter: NEAT1 knockdown induced a significant decrease of cell viability, clonogenic and migration abilities, confirming the role of this lncRNA as a critical effector of gliomagenesis. Altogether, our results suggest a complex interplay among different RNAs in GSCs: miR-370-3p shows a prominent tumor-suppressor function by targeting mRNAs involved in EMT and in hypoxia pathways (i.e., HMGA2 and HIF1A, respectively). HIF1A, in turn, regulates transcription of NT5E/CD73, which are involved in tumor development, adaption to hypoxia and promotion of immune-escape. Furthermore, the down-regulation of miR-370-3p is associated with the over-expression of the lncRNA NEAT1, which enhances cell growth and invasiveness in GBM. Understanding the lncRNA–miRNA–mRNA interplay could unveil novel applications of ncRNAs not only as diagnostic and predictive biomarkers, but also as targets of cancer therapy itself, informing the development of precision medicine and leading to new combination therapies as promising methods for GBM treatment.

INTRODUCTION

Gliomas are highly prevalent forms of brain tumor in humans, categorised into four classes based on the cellular origin: astrocytomas, oligodendrogliomas, ependymomas, and mixed tumors (Ferris et al., 2017, Ostrom et al., 2014). Additionally, gliomas are classified into four grades: grade I and II are considered low-grade gliomas and grade III and IV are considered high-grade gliomas (Banan and Hartmann, 2017). Glioblastoma (GBM) is the most common and lethal form of glioma in adults (Tanaka et al., 2013) and is classified as a grade IV astrocytoma.

GBM current gold standard treatment consists in a combination of surgical resection, radiation, and chemotherapy with temozolomide (TMZ). However, prognosis is alarmingly dismal, with a survival time of 14-15 months from the time of diagnosis, and only 5,8% of patients surviving up to 5 years post-diagnosis (Ostrom et al., 2018a, Ostrom et al., 2018b). The impact of GBM on society and health costs is greater than its relatively rare occurrence may suggest (Wirsching et al., 2016): this is due to its highest incidence around the age of professional maturity, and the deterioration of the patients' life quality, caused by neurological decline (Ostrom et al., 2014).

Novel treatments, such as immunotherapy and tumor treating fields (TTF), have been proposed as additions to the gold standard (Janjua et al., 2021). Studies to identify new drug targets have so far been unsuccessful, as targeted compounds that perform well in preclinical studies fail *in vivo* due to several factors, such as the blood brain barrier (BBB), the tumor's heterogeneity and unique immune microenvironment (Szopa et al., 2017, Shergalis et al., 2018). Heterogeneity is one of the main GBM histological characteristics and it can be expressed at different levels, including the appearance, genetic composition, and the variety of mechanisms by which it evades therapy (Baronchelli et al., 2013).

Further studies have revealed how GBM's recurrence and resistance are induced, among other factors, by a subpopulation of slow-dividing, malignant cells, displaying stem-like properties reminiscent of normal stem cells, called GBMstem-like cells (GSCs) (Singh et al., 2004, Ahmed et al., 2013). Analyses of patient-derived GSCs have identified two GSC clusters, named GSf (full stem-like) and GSr (restricted stem-like), characterised by distinct molecular signatures and phenotypes that overlap with the previously described proneural and mesenchymal GBM subtypes, respectively (Verhaak et al., 2010, Marziali et al., 2016). GSCs represent a powerful tool for *in vitro* studies because they can be isolated from the tumor to generate self-renewing, multipotent and highly tumorigenic cell lines (Gimple et al., 2019). These cells recapitulate the *in vivo* biology and functions of GBM better than other commonly

employed cell lines, to the point that they can predict the response to therapy of the original tumor, attracting further studies on their physiology and processes (Lee et al., 2006, Ernst et al., 2009, D'Alessandris et al., 2017, Gimple et al., 2019).

Thanks to the growing use of high-throughput technologies, it is known that a consistent portion of the untranslated genome, previously labeled "junk DNA", is transcribed to produce non-coding RNAs (ncRNAs). Non-coding RNAs are key regulators of both normal and pathological physiological processes, playing roles such as oncogenic drivers and tumor suppressors in many cancer types (Chan and Tay, 2018, Slack and Chinnaiyan, 2019). NcRNAs can be divided into different classes, approximately based on their size: small ncRNAs include microRNAs (miRNAs), transferRNA-derived small RNAs (tsRNAs) and PIWI-interacting RNAs (piRNAs). LncRNAs, are a heterogeneous, not fully understood group of transcripts, more than 200 nucleotides long (Esteller, 2011, Yan and Bu, 2021). Currently, studies are focused on two main ncRNAs classes, miRNA and lncRNA, due to their impressive ability to influence gene regulation in a very refined and efficient way across all cellular physiological pathways in mammals and humans (Chi et al., 2019, Hill and Tran, 2021, Woods and Van Vactor, 2021).

LncRNAs are functionally categorised as signalling, decoy, guide, and scaffold lncRNAs and are involved at multiple levels in gene expression, growth, differentiation, and development (Engreitz et al., 2016, Bhan et al., 2017). LncRNAs have cell-specific and time-specific expressions, serving as a response to various stimuli (Mahinfar et al., 2021). While most lncRNAs are in the nucleus, they can also have functional roles in cytoplasm, and can even be transmitted to other cells or serum through exosome tracking (Chi et al., 2019).
Furthermore, several lncRNAs are oncogenes, while others act as oncosuppressors: genome-wide association studies of tumor samples have found that alterations in lncRNA expression are involved in many types of cancer (Schmitt and Chang, 2016, Bhan et al., 2017).
LncRNAs can also interact with other ncRNAs: in fact, some lncRNAs have complementary sites for miRNAs, known as "miRNA response elements" (MRE), which protect transcripts by making miRNA binding sites on mRNAs inaccessible, effectively acting as miRNA "sponges" (Bhan et al., 2017, Anastasiadou et al., 2018).

Recently, microarray studies found an example of the consequences of altered lncRNAs expression in tissues of different subtypes of glioma and in normal brain tissue (Zhang et al., 2012a). Intriguingly, it is the

lncRNA NEAT1 (Nuclear Enriched Abundant Transcript 1), normally crucial for the formation of paraspeckles, that also serves an oncogenic function in gliomas, regulated by the EGFR pathway and contributing to tumor growth and invasiveness (Chen et al., 2018b, Shan et al., 2020). NEAT1 acts at post transcriptional level by sponging oncosuppressive miRNAs, which then lose their function in favour of oncogenic mRNAs (Bartel, 2009).

MicroRNAs (miRNAs) are a class of short RNAs (20-23 nt) which act at post-transcriptional level regulating gene expression by blocking mRNA translation and/or stability. Transcripts are targeted through MRE, a short 7-nt seed sequence within the miRNA. MREs binding does not have to be perfectly complementary, which makes difficult predicting miRNA targets (Dong et al., 2013, Dykes and Emanueli, 2017).
MiRNAs are known to be implicated in almost every facet of the development and malignant progression of gliomas, including maintenance of the stemness of GSCs, invasiveness, angiogenesis, epigenetic regulation, and signaling pathways (Chan et al., 2005, Mizoguchi et al., 2012, Mizoguchi et al., 2013, Zeng et al., 2018).

Some reports also indicate the association of miRNA dysregulation with GBM resistance to standard chemotherapy with (TMZ) (Shi et al., 2010, Ujifuku et al., 2010, Zhang et al., 2012b). Further analyses in GSCs have found that miRNA expression is significantly downregulated compared to normal neural stem cells NSCs (Aldaz et al., 2013, Sana et al., 2018). These miRNAs originate mainly from a large cluster on chromosome 14 (14q32), located within a chromosomal region named DLK1-DIO3, that is known to be a cancer-associated genomic region (Benetatos et al., 2013).

MiR-370-3p is a miRNA belonging to DLK1-DIO3 domain. Several studies reported that downregulation of miR-370-3p is involved in tumorigenicity in various forms of cancers such as oral squamous carcinoma (Chang et al., 2013), hepatocellular carcinoma (Xu et al., 2013), acute myeloid leukemia (Zhang et al., 2012b), and ovarian cancer (Chen et al., 2014). In addition, studies reported that up-regulation of miR-370-3p is implicated in the progression of prostate cancer (Wu et al., 2012), gastric carcinoma (Lo et al., 2012) and Wilms tumor (Cao et al., 2013). Moreover, miR-370-3p expression was frequently found decreased in glioma tissues, particularly in recurrent GBM (Gao et al., 2016, Chen et al., 2018a, Chen et al., 2019). Furthermore, this miRNA may act as oncosuppressor in glioma by inhibiting cell proliferation (Peng et al., 2016). However, the full biological role and functional mechanisms of

miR-370-3p are not fully clarified. Studies demonstrated that both lncRNAs and miRNAs could act as oncogenes and/or tumor suppressors (Bhan et al., 2017, Bartonicek et al., 2016), affecting initiation and progression of many types of cancer, including gliomas (Shi et al., 2017, Yan et al., 2017).

New studies are increasing our knowledge on the mechanism involved in miRNA targeting and their various interaction partners (e.g. lncRNAs), and the hypothesis of a reciprocal regulation is emerging (Chan and Tay, 2018).

Overall, our study of the role of lncRNAs and their interactions with miRNAs has deepened our understanding of GBMs, and more importantly, has helped characterising their role in the proliferation and invasiveness of GSCs, hoping to unveil novel diagnostic and therapeutic targets.

RESULTS

MiR-370-3p is down-regulated in GBM and patient-derived GSCs

The first step we took in order to clarify the role of miR-370-3p in GBM, was analysing its expression by Real-Time PCR (RT-PCR) in 12 human GBM tissues and 27 GSCs lines derived from GBM surgical specimens. We found that the relative expression of miR-370-3p was down-regulated up to two orders of magnitude both in GBM tissues ($p < 0.0006$, Student's t-test) and GSCs lines ($p < 0.0083$, Student's t-test), when compared to our normal brain tissues ($n = 12$) and normal NSCs ($n = 5$) controls, respectively (Figure 1). These results are in line with previous works that show the dysregulation of miR-370-3p in various tumors and in GBM; the next step was therefore the search for a confirmation of its role in the GBM pathological context.

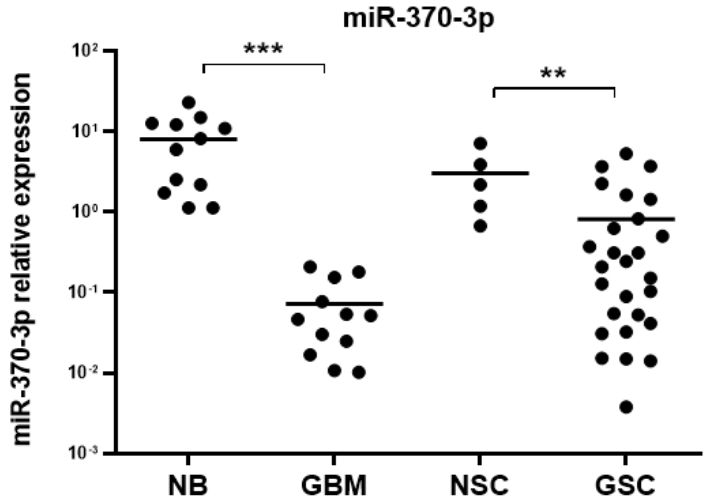

Figure 1. MiR-370-3p is downregulated in GBM tissues and GSCs lines. Real time RT-PCR analysis of miR-370-3p expression performed on samples of normal brain tissue (NB, *n* = 12), GBM tissues (GBM, *n* = 12), neural stem cells (NSC *n* = 5) and Glioblastoma stem-like cells (GSC, *n* = 27). Samples were run in duplicate and normalized with Glyceraldehyde-3-Phosphate Dehydrogenase (GAPDH). * $p < 0.05$; ** $p < 0.01$; *** $p < 0.001$. MiR-370-3p is significantly downregulated in GBM tissues and GSCs, compared to the control tissues samples and cell lines.

Restoration of miR-370-3p Impairs Cell Viability of GSCs

After confirming the dysregulation of miR-370-3p in GBM, we decided to test the impact of its restored expression on GSCs lines. Thus, we selected four GSC lines (#1, #61, #83, and #163) among the ones analyzed for miR-370-3p expression and transduced them by using an inducible Tet-On lentiviral vector (TRIPZ) carrying pri-miR-370 in the 3'-untranslated region of Red Fluorescent Protein (RFP). After being transduced, all the lines were exposed to doxycycline to induce the expression of the miRNA. The RFP-positive cells were flow-sorted and we confirmed the successful miR-370-3p restoration using real-time PCR once again. All the transduced GSCs lines showed an increase in miR-370-3p native expression levels, when compared to control vector (TRIPZ)-transduced cells, and comparable to normal cells (Figure 2A). The newly increased expression of miR-370-3p impaired cell viability in all the GSCs lines that we tested: cell numbers started to decline significantly after two to four days, suggesting that miR-370-3p could play a tumor suppressive role in GBM (Figure 2B).

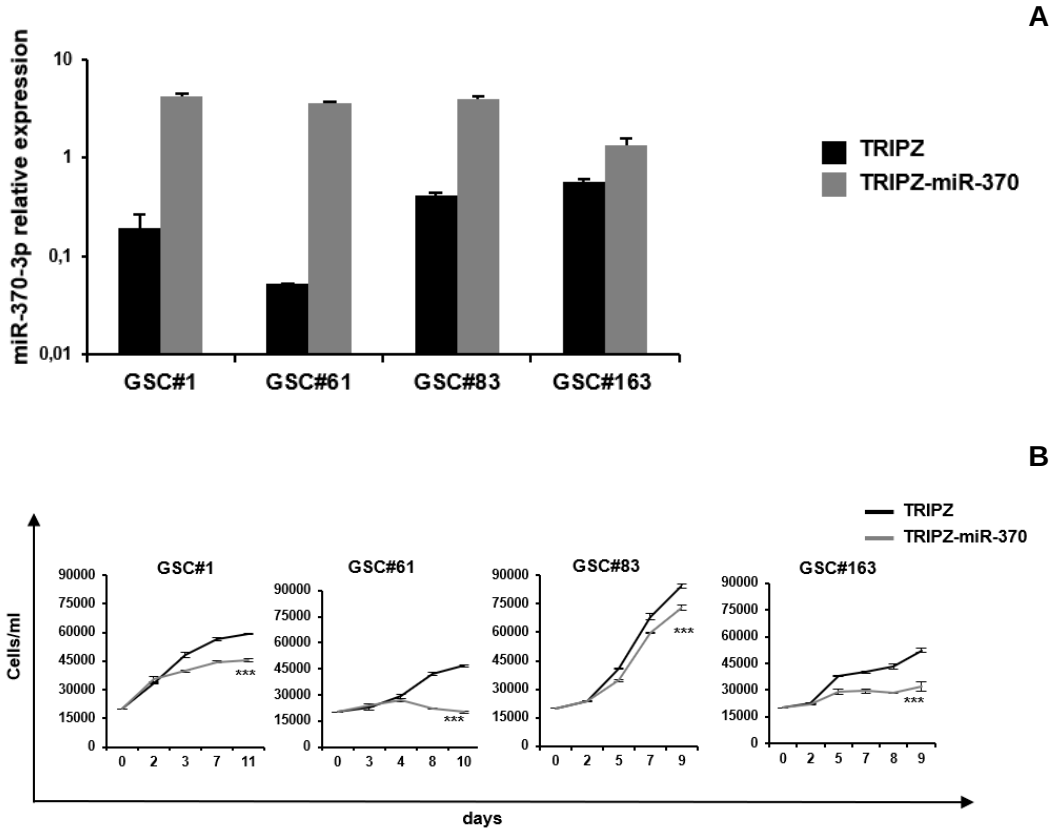

Figure 2. Restoration of miR-370-3p Impairs Cell Viability of GSCs. (A) Real time PCR analysis of miR-370-3p expression in GSC#1, #61, #83 and #163 transduced with either TRIPZ or TRIPZ-miR-370 inducible vectors. As is shown, all the TRIPZ-miR-370-transduced GSC lines showed miR-370-3p expression levels increased when compared to control vector (TRIPZ)-transduced cells. **(B)** Growth curves of GSCs transduced with either TRIPZ or TRIPZ-miR-370 vector. Points and range lines at each day represent mean and ± SD of at least two independent experiments in triplicate. Two-way analysis of variance for repeated measures was performed on the whole set of data. The restored expression of miR-370-3p significantly impaired cell viability of all the GSC lines tested, as shown by the decrease in cell number over time.

Restoration of miR-370-3p Alters Malignant features of GSCs

Seeing the evidence of the impact of restored miR-370-3p expression on GSCs viability, we decided to examine whether it could alter additional malignant features of GSCs, such as migration. After miR-370-3p restoration and induction, we tested the motility of transduced GSCs via a migration assay in a Multiwell Inserts System. We examined the fluorescence signal of migrated cells and observed a reduction in the migration capabilities of TRIPZ-miR-370 transduced GSCs of at least 20% and up to about 40% (Figure 3A). As an additional test, we analyzed the clonogenic capability of GSC expressing miR-370-3p. Doxycycline-induced GSCs were plated as single cells in 96-well plates in triplicate and allowed to grow for two weeks. Again, TRIPZ-miR-370-transduced GSCs formed up to 30% fewer colonies as compared to TRIPZ cells (Figure 3B).

Thus far, the restoration of miR-370-3p has resulted in the inhibition of several of the GSCs worse tumorigenic characteristics, reinforcing the hypothesis that this miRNA can play a pivotal role in GBM oncosuppression.

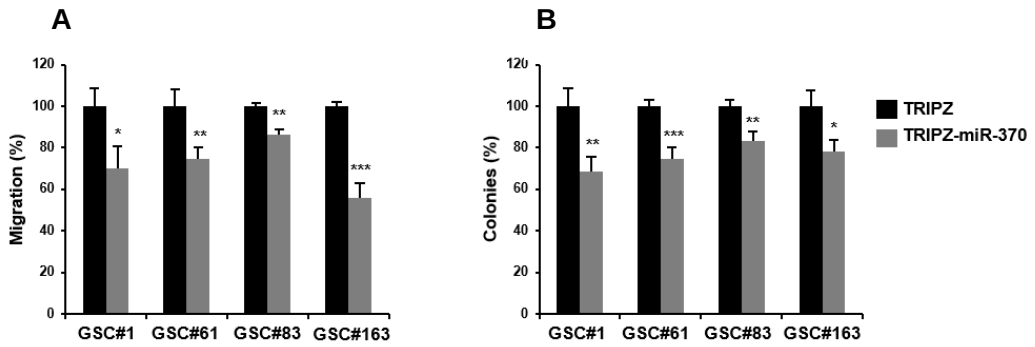

Figure 3. Restoration of miR-370-3p Alters Malignant features of GSCs. (A) Analysis of migration efficiency in GSCs transduced with TRIPZ-miR-370 vector 48 h after induction. Values are reported as percentage relative to control vector and shown as mean ± SD from two independent experiments in triplicate. As shown by the graphic, a dramatic reduction in the migration capabilities of TRIPZ-miR-370 transduced GSCs, was observed **(B)** Analysis of efficiency in colony formation of GSCs after transduction with TRIPZ-miR-370 vector. Efficiency in colony formation in TRIPZ transduced cells, ranging from 20% to 30%, was used as reference. Percent colony number values from two independent experiments in triplicate were calculated over the correspondent empty vector and are shown as mean ± SD for each GSC line. TRIPZ-miR-370 transduced GSCs formed significantly fewer colonies as compared to TRIPZ cells.

Restoration of miR-370-3p Inhibits Tumor Growth *in vivo* in an Orthotopic Xenograft Mouse Model

To further corroborate our promising *in vitro* results, we decided to investigate the effects of miR-370-3p restoration on GBM growth *in vivo.* We used orthotopic injection of patient-derived GSCs in immunocompromised mice to continue our analysis, because through this model it is possible to generate tumors that are highly infiltrative and closely mimic the parent neoplasm (D'Alessandris et al., 2017). This time, the TRIPZ and TRIPZ-miR-370-transduced GSCs were also transduced with a lentiviral vector expressing a green fluorescence protein (GFP), to help trace the grafted GSCs after the injection.

We used a total of 6 mice: a control group (*n*, 3) was grafted with GSC#1 cells containing the empty TRIPZ vector, while the second group (*n*, 3) was grafted with TRIPZ-miR-370-transduced GSC#1. The model we used is so stable and reproducible that we were able to limit the number of mice to three for each group.

After four weeks, the control group mice had developed tumors that invaded the injection site in the striatum, the homolateral piriform cortex, and managed to spread into the contralateral paraventricular area through the corpus callosum (Figure 4A-C). On the other hand, in mice grafted with TRIPZ-miR-370-transduced GSC#1 the degree of brain invasion of the injected striatum was significantly reduced and no migration of GSCs to the contralateral hemisphere was observed (Figure 4D-F, I, J). We also observed a reduction of the brain volume invaded by tumor cells in the mice grafted with TRIPZ-miR-370-transduced GSC#1 cells: 34.89 × 106 ± 8.49 μ/m3 (p = 0.027, Student-*t* test), versus 133.54 × 106 ± 20.50μ/m3 (mean ± sem) in control mice.

The logical next step was to assess whether miR-370-3p has an impact on GSCs *in vivo* proliferation as well. We used the Ki67 labeling index to mark the proliferating cells in both groups of mice. The results showed that proliferation of tumor cells was higher in the control group xenografts (23.78 ± 1.99%) than in the TRIPZ-miR-370-transduced GSC#1 grafts (10.56 ± 0.88%) ($p < 0.0001$; Student-t test; Figure 5A-D). We obtained the percent colony number values from two independent experiments in triplicate, calculated over the corresponding empty vector and are shown as mean ± SD for each GSC line.

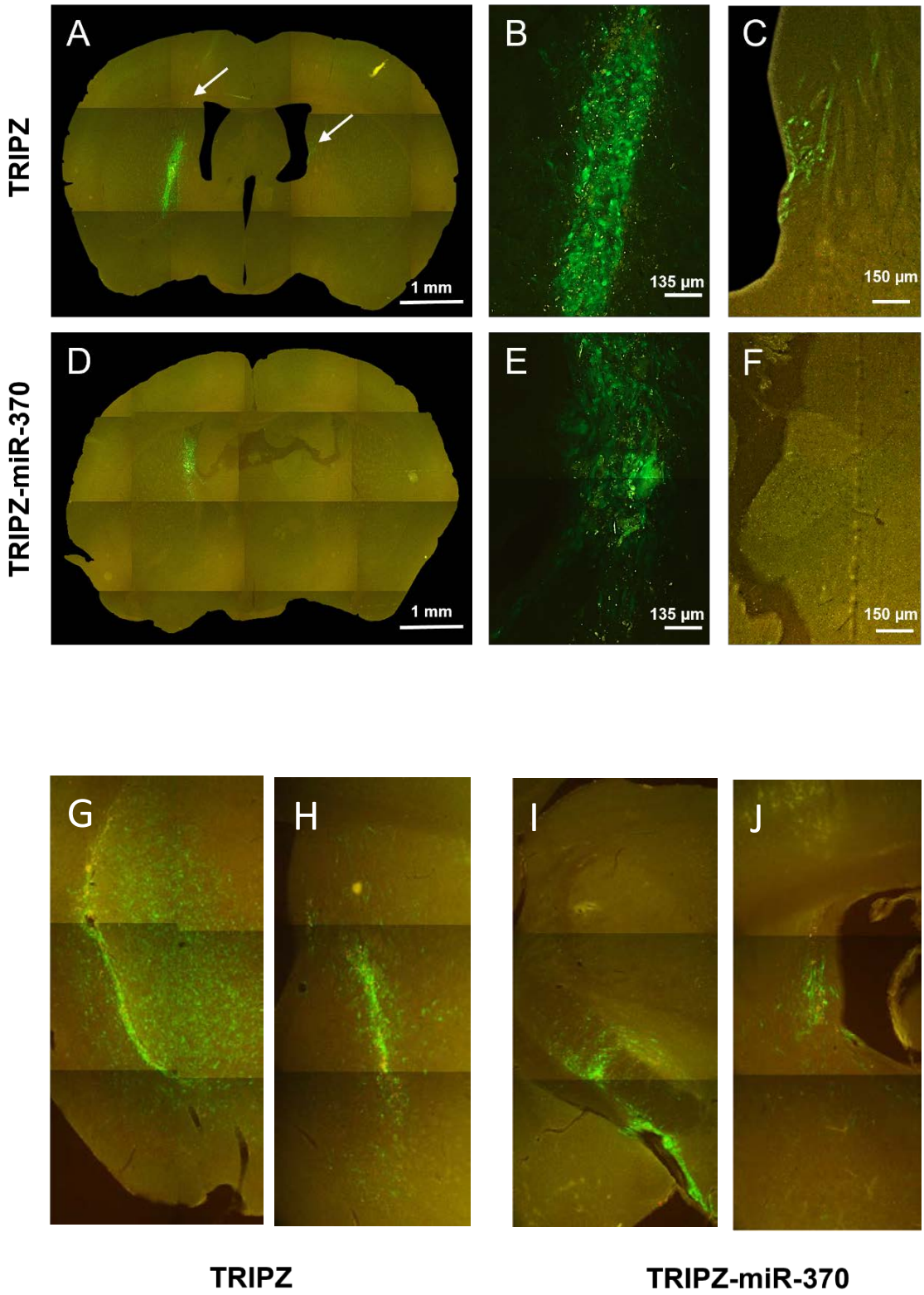

Figure 4. Restoration of miR-370-3p inhibits tumor growth in orthotopic xenograft mouse models.
Fluorescence microscopy of mouse brain grafted onto the right striatum with GSC#1 cells. *Upper panel* **(A-C)**, coronal section of TRIPZ xenograft showing the injection area and tumor spreading to the subventricular zone of the contralateral hemisphere. The arrows point to tumor cells. *Lower panel* **(D-F)**, Photomontage of coronal section in a TRIPZ-miR-370 xenograft. A few tumor cells with cell debris are found in the injection area **(E)**. There is no contralateral spreading of tumor cells. **(G-H)** Detailed photomontage of coronal section of a TRIPZ xenograft and of a TRIPZ-miR-370 xenograft **(I-J)** showing injection area. Scale bars, 200 µm.

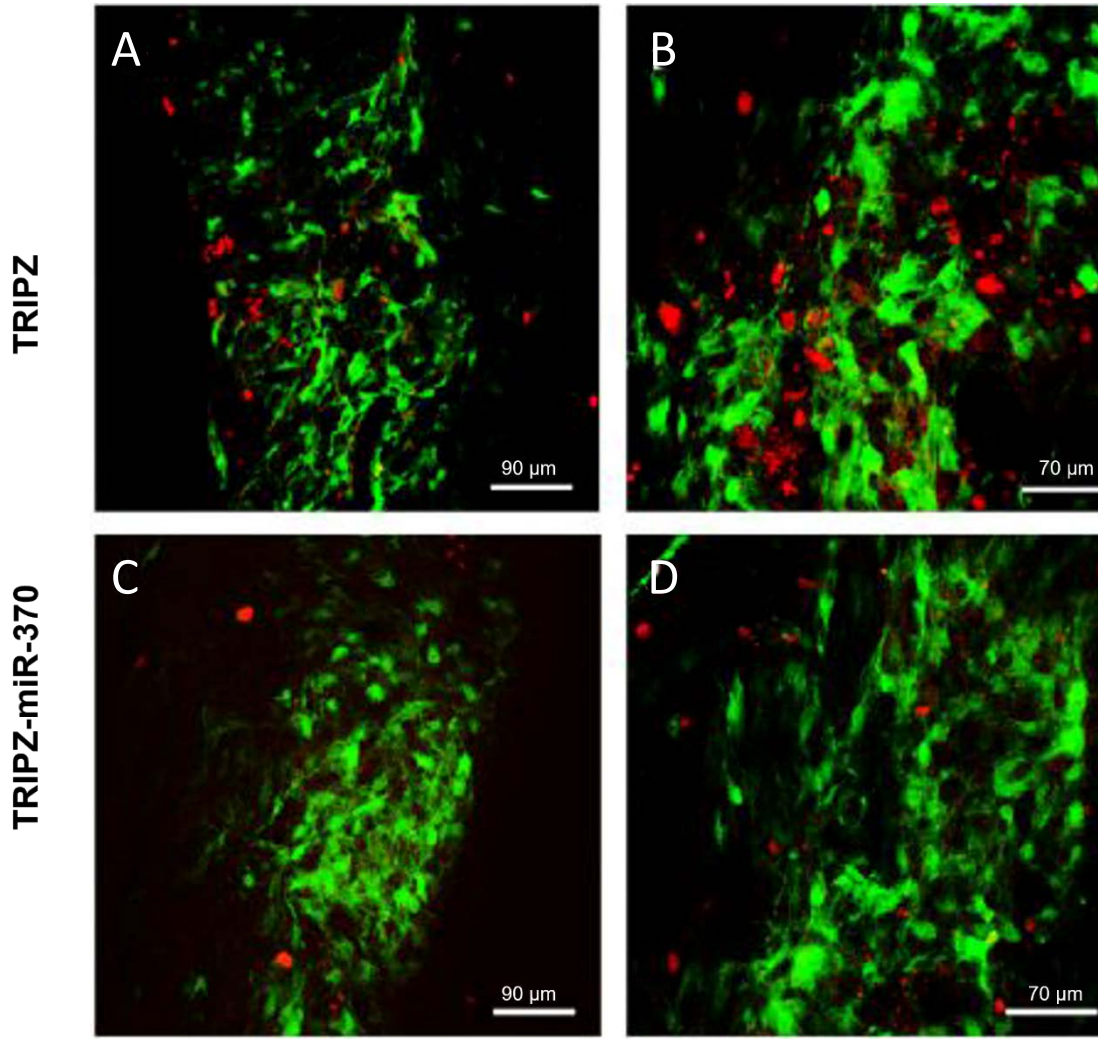

Figure 5 Ki67 immunostaining showing positive nuclei of proliferating cells (red) in a TRIPZ xenograft **(A–B)** and in a TRIPZ-miR-370 xenograft **(C–D)**.

Tumor Suppressor Function of miR-370-3p induces Inhibition of EMT

With evidence of the oncosuppressing role of miR-370-3p piling up, we turned our attention to deepening our understanding of the regulatory networks and mediators of miR-370-3p functions.
Therefore, we analyzed by microarray the gene expression profiles of GSCs transduced either with TRIPZ-miR-370 or TRIPZ empty vector, with the aim to find the most deregulated genes. We then used the Gene Set Enrichment Analysis (GSEA) software (https://www.gsea-msigdb.org/gsea/index.jsp) to compare our molecular profile data with the Molecular Signature DataBase (MSigDB), a collection of annotated

gene sets, to detect significant variations in gene networks (Subramanian et al., 2005, Mootha et al., 2003). We restricted our results to transcripts either up- or down-regulated at least two-fold in the miR-370-3p transduced GSCs, to highlight the most enriched pathways. Thanks to the functional annotation-clustering tool we were able to analyse 836 unique identifiers corresponding to dysregulated transcripts, thus identifying 81 genes assigned to pathways enriched with a p-value below 0.001. Among these, the results indicate that the most significantly enriched pathways were those related to EMT and hypoxia (Figure 6A, Supplementary Table 2).

We used the TargetScan 6.2 and microRNA.org algorithms (www.targetscan.org, http://www.microrna.org/microrna/home.do) to search for potential mRNAs targeted by miR-370-3p among the dysregulated transcripts. One such target was the high-mobility AT-hook 2 (HMGA2) group, which belongs to the high-mobility group (HMG) protein family. The targeting of HMGA2 by miR-370-3p was previously described in the context of non-functional pituitary adenoma, and the HMGA2 group is known to function as an oncogene and EMT inducer in several types of human cancer (Liu et al., 2014, Cai et al., 2019). We found that the restoration of miR-370-3p induced a ~40% decrease of HMGA2 expression in each GSC line we analyzed, evidencing the presence of this interaction also in GBM pathological context (Figure 6B, left panel).

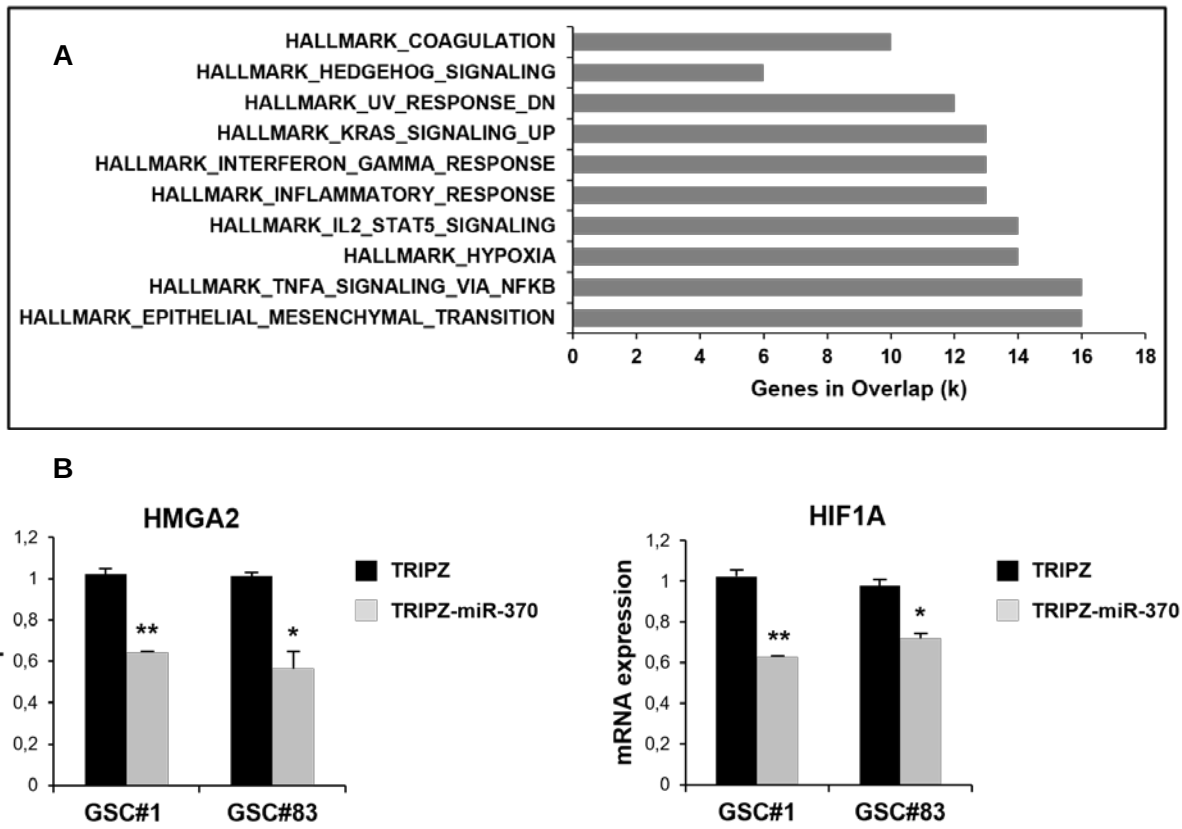

Figure 6. Effect of miR-370-3p restoration in GSCs. (A) Pathway enrichment analysis examined by GSEA software of highly modulated genes (≥2 fold both up and down) in GSC#1 transduced with TRIPZmiR-370 vs TRIPZ empty vector. **(B)** RT-PCR analysis performed on GSC#1 and GSC#83 transduced with TRIPZ or TRIPZ-miR-370 for HMGA2 *(*left panel*)* and Hypoxia-inducible factor (HIF) 1A expression *(*right panel). * $p < 0.05$; ** $p < 0.01$.

Tumor Suppressor Function of miR-370-3p in Response to Hypoxia in GSCs

Among other potential miR-370-3p targets, we found the Hypoxia-Inducible Factor (HIF) 1A. When we restored the expression of miR-370-3p in GSCs with TRIPZ-miR-370, the expression level of HIF1A was 30 to 40% reduced, if compared to TRIPZ empty vector cells (Figure 6B, right panel).

In light of this promising result, we performed a dual-luciferase reporter assay to test whether miR-370-3p directly targets HIF1A. We used wild type (wt) HIF1A and mutant (*mut*) HIF1A vectors for the assay: the results show a significant reduction (~40%) in the luciferase activity only for the wt HIF1A, confirming the predicted miR-370-3p-HIF1A direct interaction (Figure 7A, right panel).

Interestingly, continuing our search we found that not every dysregulation is proof of a direct interaction. In fact, NT5E/CD73, an enzyme responsible for adenosine (ADO) production, was found among the most significantly down-regulated genes in miR-370-3p restored GSCs. We assessed its expression by flow cytometry and found it was reduced in TRIPZ-miR-370-transduced GSCs compared to TRIPZ empty vector cells (Figure 7B), but failed to be among the direct targets of miR-370-3p in a dual luciferase assay. Despite this, it is known that CD73 down-regulation has indeed an impact in glioma, decreasing cell migration and invasion; in addition, the knockdown of CD73 potentiated TMZ cytotoxic effects on glioma cells, decreasing the IC50 value and sensitizing the cells to a non-cytotoxic drug concentration (Azambuja et al., 2019). Thus, our results suggest that miR-370-3p may indirectly modulate the expression of CD73 by its direct interaction with HIF1A. Indeed, HIF1A directly binds to the NT5E promoter and thereby activates the expression of CD73 (Synnestvedt et al., 2002, Colgan et al., 2006).

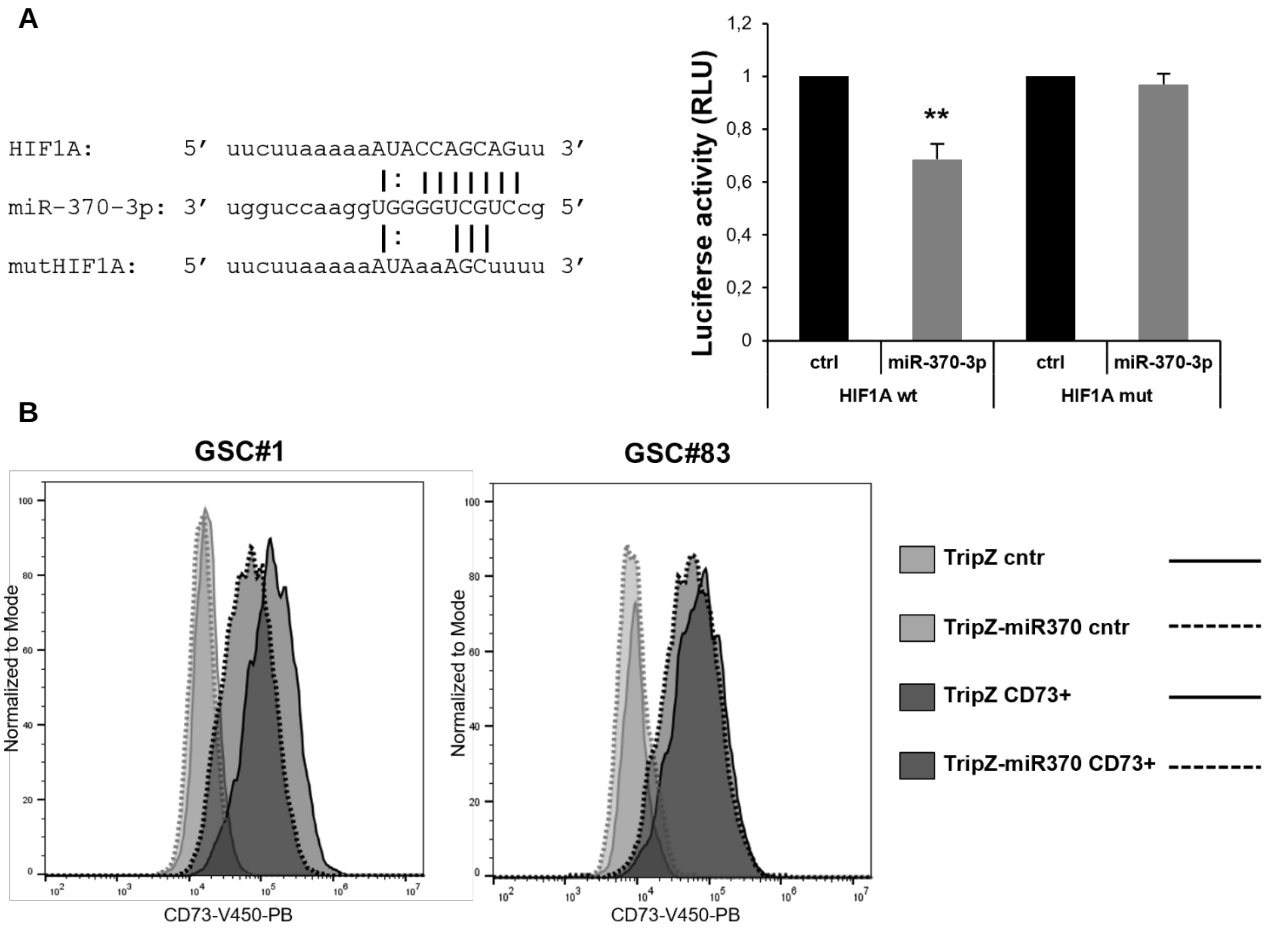

Figure 7. MiR-370-3p target prediction. (A) Predicted binding site of miR-370-3p in the HIF1A 3'UTR sequence (left panel). Dual-luciferase of pGL3 vectors containing the HIF1A 3'UTR or HIF1A mutant (mut), co-transfected in 293T cells with hsa-miR-370-3p-mimic or control mimic RNA (ctrl). ** $p < 0.01$. Histograms show normalized mean values of the relative luciferase activity. Error bars represent the mean $\pm$ SD (n = 4) (right panel) **(B)** FACS analysis of NT5E/CD73 on GSC#1 and GSC#83 transduced with TRIPZ empty vector and TRIPZ-miR-370 after doxycycline induction. The faint lines and light grey areas are referred to the control antibody signal.

MiR-370-3p Interacts with lncRNA NEAT1

After our analyses of the interactions between miR-370-3p and mRNAs, we turned our attention to non-coding RNAs, since studies confirm that miRNAs and lncRNAs can interact in a sequence-specific manner (Ballantyne et al., 2016). We used starBase v2.0, an online repository of RNA known interactions, to identify lncRNAs with complementary base pairing with miR-370-3p (http://starbase.sysu.edu.cn) (Li et al., 2014). Among the list of lncRNAs possibly interacting with miR-370-3p, we decided to focus on Nuclear Enriched Abundant Transcript 1 (NEAT1) for further investigation: NEAT1 is linked to hypoxia, promotes EMT, and correlates with higher WHO classification for human glioma (Zhang et al., 2017, He et al., 2016, Kong et al., 2019). The direct interaction between NEAT1 and miR-370-3p was predicted to happen in two seed sequences (chr11:65191743-65191764[+] and chr11:65196739-65196760[+]) at +1500 and +6500 nucleotides of the RNA sequence, respectively, so we performed dual-luciferase reporter assays to test the binding (Figure 8A). We prepared two groups of 293T cells, one with miR-370-3p mimics and a control group with non-targeting control RNA (ctrl). We then co-transfected cells from both groups with wild type (wt) NEAT1 and mutant (*mut*) NEAT1 reporter vectors.

We observed a 30 to 40% reduction of the luciferase activity in the cells with the miR-370-3p mimic and transfected with the wt NEAT1, both for NEAT1(+1500) and for NEAT1(+6500); on the other hand, no significant changes were observed for the mut NEAT1 reporter constructs in either of the seed sequences (Figure 8B), confirming the direct interaction between the two ncRNAs.

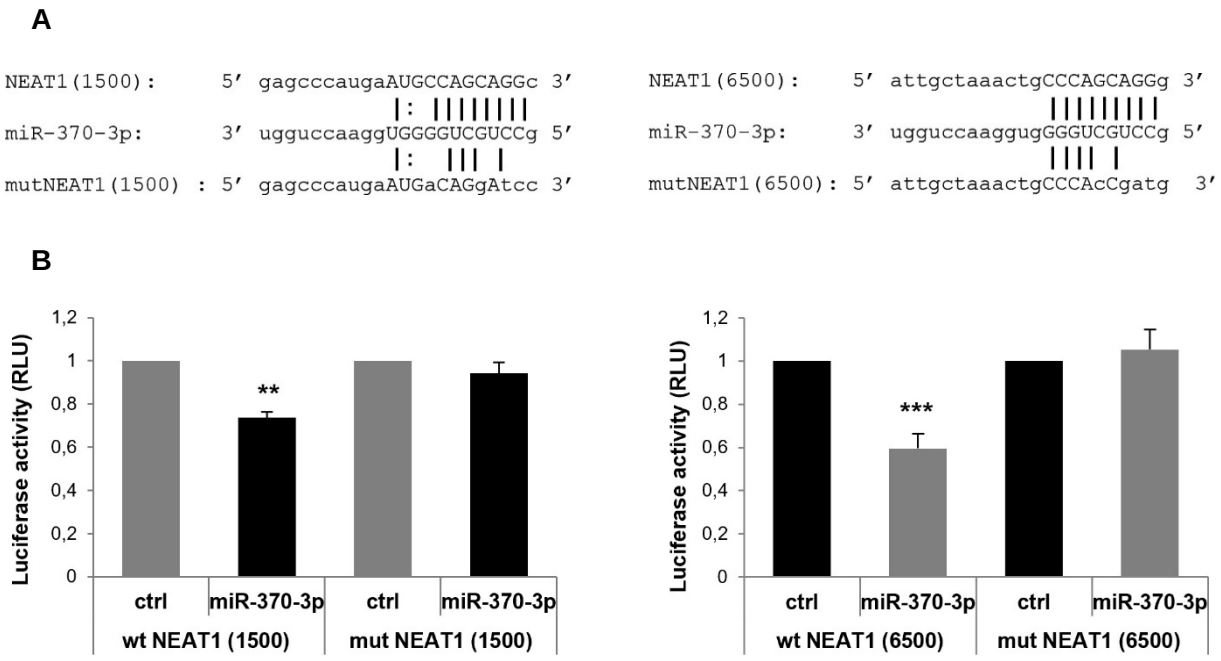

Figure 8 MiR-370-3p Interacts with lncRNA NEAT1. (A) Binding sites between miR-370-3p and NEAT1 at +1500 (left panel) and at +6500 (right panel) nucleotides of RNA sequence. **(B)** Dual-luciferase reporter assays in 293T cells co-transfected with reporter vectors containing the wild type (wt) or the mutated (mut) NEAT1(1500) (left panel) or NEAT1(6500) (right panel) sequences and miR-370-3p-mimic or control mimic RNA (ctrl). Bar charts show normalized mean values of the relative luciferase activity. Error bars correspond to the mean ± SD (n = 4) (student t-test: ** $p < 0.01$; *** $p < 0.001$).

MiR-370-3p and NEAT1 Expression is Inversely Correlated in GBM Tissues and GSC Lines

In an effort to improve our understanding of the interaction between miR-370-3p and NEAT1, we examined the NEAT1 expression levels in the same cohort of samples previously utilised to investigate the expression levels of miR-370-3p, i.e. the 12 human GBM tissues and 27 GSC lines, compared once again to 12 normal brain tissues and 5 normal NSCs. Unsurprisingly, the expression level of NEAT1 was up to an order of magnitude higher in GBM tissues ($p < 0.0001$, Student's t-test) and GSCs ($p < 0.017$, Student's t-test) compared to normal brain tissues and normal NSCs, respectively (Figure 9A). Therefore, it's worth pointing out that miR-370-3p and NEAT1 seem to be under a reciprocal regulation: their expression levels are inversely correlated in both GBMs (Figure 9B) and GSCs (Figure 9C) (Spearman correlation coefficient 0.63 and 0.22, $p < 0.006$ and $p < 0.01$, respectively). We searched the dataset of The Cancer Genome Atlas (TCGA) (http://starbase.sysu.edu.cn/starbase2/) for correlations between these

two ncRNAs in GBM but, unlike a number of other types of tumors, like urothelial bladder cancer (r = -0.26), head and neck squamous cell carcinoma (r = -0.29), acute myeloid leukemia (r = -0.18), we did not find significant correlations.

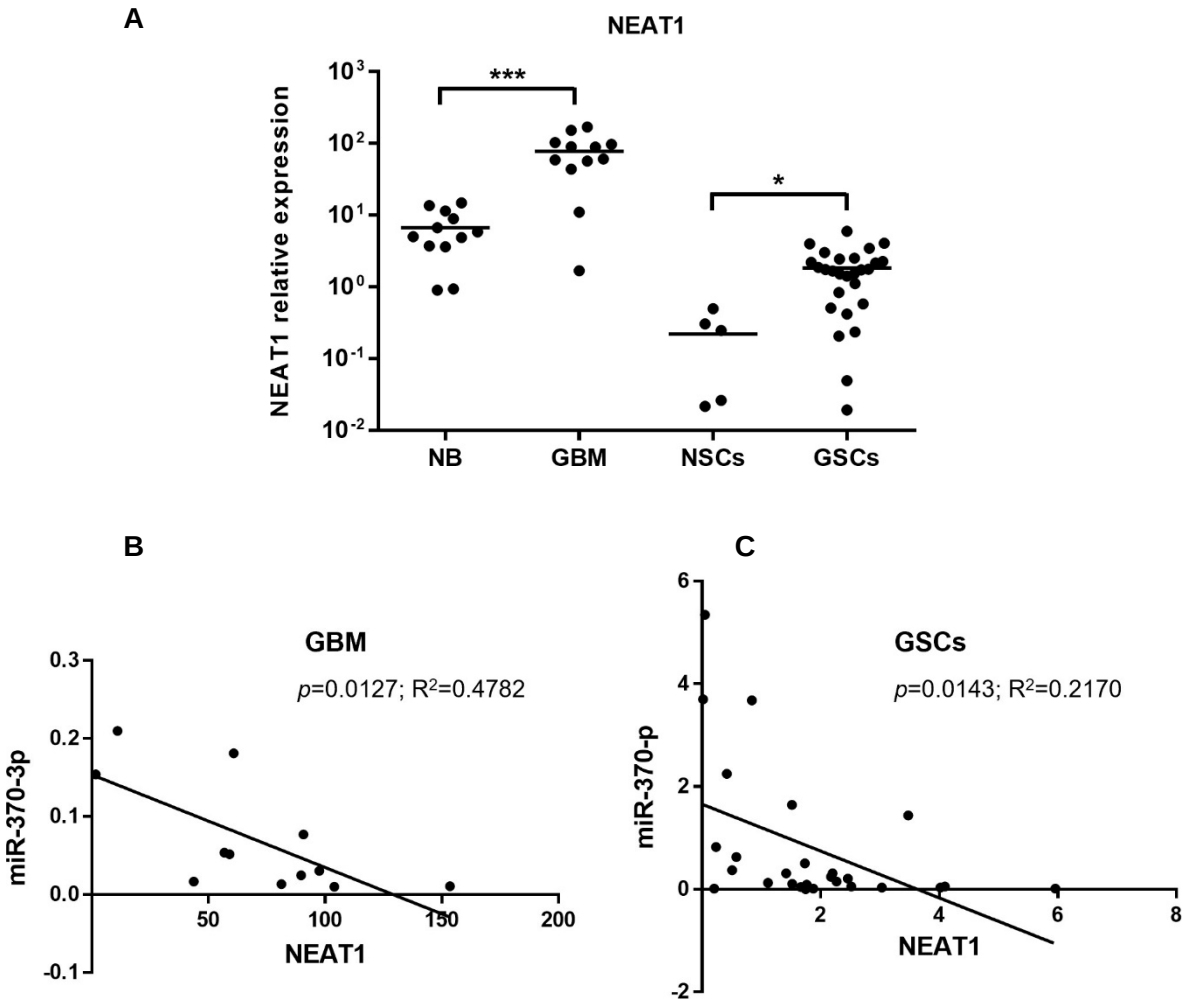

Figure 9 MiR-370-3p and NEAT1 Expression is Inversely Correlated in GBM Tissues and GSCs. (A) RT-PCR analysis performed on normal brain samples (NB, n = 12), GBM tissues (GBM, n = 12), NSCs (n = 5) and GSCs (n = 27). Samples were run in duplicate and normalized with GAPDH. * p < 0.05; ** p < 0.01; *** p < 0.001. **(B)** Correlation analysis between miR-370-3p and NEAT1 expression levels in GBM tissues and in GSC lines**(C)**.

NEAT1 knockdown impairs GSC viability, migration and clonogenic ability, through its interaction with miR-370-3p

After proving the reciprocal regulation of the expression of miR-370-3p and NEAT1, we decided to check the expression levels of NEAT1 in two of our GSCs cell lines (GSC#1 and GSC#83) after the restoration of miR-370-3p. As expected, miR-370-3p restoration induced a 40 to 80% down-regulation of NEAT1, further confirming a direct interaction between the two non-coding RNAs (Figure 10A).

We then examined the possible additional effects of NEAT1 silencing by mirroring the approach previously used for miR-370-3p. We transduced the GSC#1 and GSC#83 lines with lentiviral vectors carrying short hairpin (sh)NEAT1 or shNTC (no target control) sequences and green fluorescent protein (GFP) as a reporter. After transduction, the GFP-positive cells of both lines showed a decrease in excess of 40% for the endogenous levels of NEAT1, with comparable decreases for HIF1A and HMGA2 and an overexpression of miR-370-3p (Figure 10B).

We then evaluated the *in vitro* effects of NEAT1 silencing on viability, clonogenic ability and migration.

As expected, NEAT1 knockdown induced a significant and steady decrease of cell viability from day 1 (GSC#1) or day 5 (GSC#83) (Figure 10C).

We performed a colony formation assay to analyze the clonogenic ability of the GSCs lines: shNEAT1 and shNTC transduced GSCs were plated and grown as single cells. We found a reduced clonogenic ability (20 to 40% less) for stably NEAT1-silenced GSCs of each line, when compared to the shNTC GSCs (Figure 10D).

In the same context, a migration assay performed in the FluoroBlok™ Multiwell Inserts System showed a decrease of comparable magnitude in the migration capabilities of the NEAT1-silenced cells, compared to shNTC cells (Figure 10D), confirming the role of this lncRNA as a critical effector of glioma development.

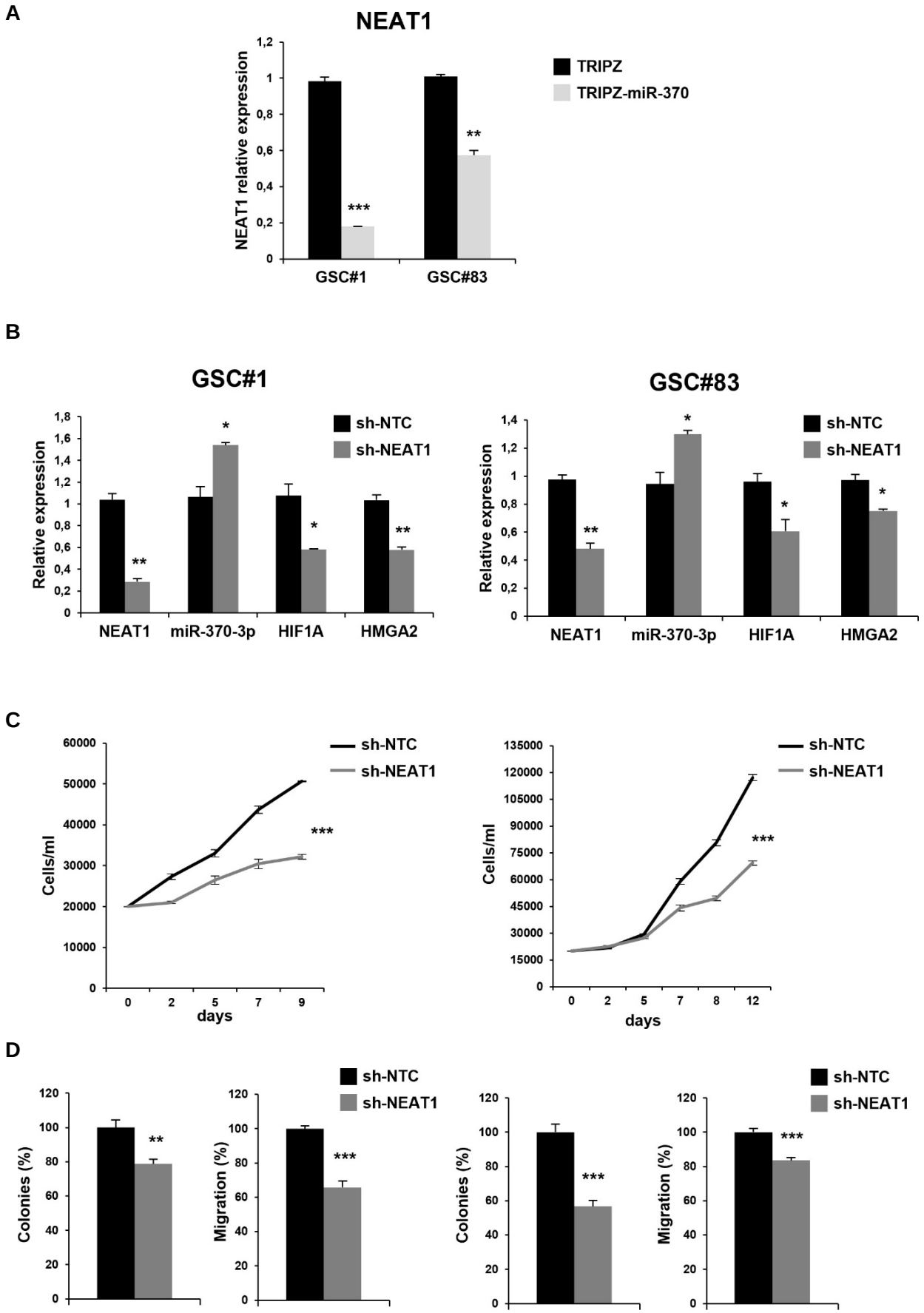

Figure 10 NEAT1 knockdown impairs GSC tumorigenicity. (A) Real time PCR analysis for NEAT1 on GSC#1 and GSC#83 miR-370-3p transduced lines confirmed the downregulation of the lncRNA (** $p < 0.01$; *** $p < 0.001$). **(B)** Real time PCR for NEAT1, miR-370-3p, HIF1A and HMGA2 on GSC#1 (left panel) and GSC#83 (right panel) transduced with short hairpin (sh)NEAT1 or its no target control lentiviral vector (shNTC) (* $p < 0.05$; ** $p < 0.01$. **(C)** Growth curves of GSCs lines transduced, **(D)** analysis of efficiency in colony formation and analysis of migration efficiency in GSC#1 (left panel) and GSC#83 (right panel) transduced with shNEAT1 or shNTC. Values shown are mean ± SD from two independent experiments in triplicate (** $p < 0.01$; *** $p < 0.001$).

Patients with High miR-370-3p and low NEAT1 expression levels show an improved survival rate

Once we uncovered the miR-370-3p-NEAT1 reciprocal regulation, we tested what relationship there may be between their expression and patient survival. We took the expression levels and survival data for the GBM patients from which the GSCs we analysed are derived, and found that the expression level of miR-370-3p was not associated with prolonged value for survival ($p = 0.0911$; Hazard Ratio (HR) 0.4778; 95% CI from 0.2029 to 1.1253), while high NEAT1 expression was indeed associated to unfavorable overall survival (OS) ($p = 0.035$; HR 2.7980; 95% CI from 1.0754 to 7.2804), in line with previously published results (He et al., 2016) (Figure 11A,B).

To broaden the scope of our analysis, we tested the relationship between miR-370-3p and NEAT1 expression levels with the survival rates of patients in the TCGA database. We employed a risk stratification model to derive the Kaplan–Meier curve for Overall Survival (OS) in GBM TCGA patients, stratified for low miR-370-3p/high NEAT1 vs. high miR-370-3p/low NEAT1 (Figure 11C). The high miR-370-3p/low NEAT1 group seems to be associated with a slight improvement of the survival time, for all survival probabilities. The last group of the analysis was associated with an anomalously better survival outcome, exceeding 2500 days for patients with high miR-370-3p/low NEAT1 ($p = 0.0215$, HR 0.6855, 95% CI from 0.4968 to 0.9458). We decided to perform an additional analysis, this time including the expression levels of HIF1A in the stratification model: the new Kaplan–Meier curve for OS in GBM TCGA patients was then stratified for low miR370-3p/ high NEAT1/ high HIF1A vs. high miR370-3p/ low NEAT1/low HIF1A ($p = 0.4400$, HR 0.7927, 95% CI from 0.4395 to 1.4296) (Figure 11D). The resulting graph shows that the last subgroup is not correlated to a significantly better prognosis anymore, although there is an association between patients with longer survival times and high miR370-3p/ low NEAT1/low HIF1A.

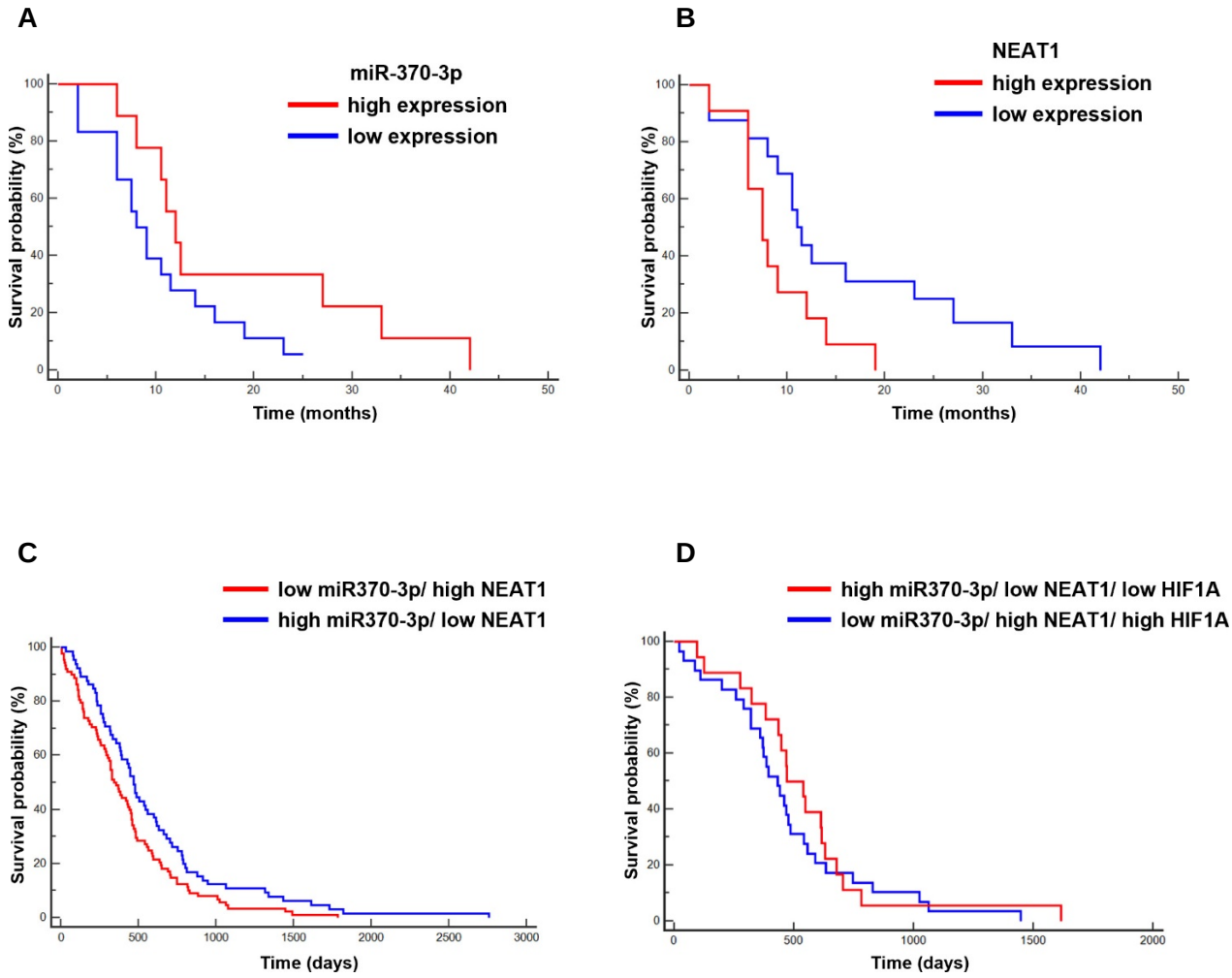

Figure 11 MiR-370-3p and NEAT1 Inversely Correlated Expression is associated with overall survival (OS) in GBM. (A) Kaplan–Meier curve for OS in our cohort of GBM patients stratified for low miR-370-3p expression (<the median value) vs high miR-370-3p expression (>the median value). The last group was not associated to a better outcome (n = 27, p = 0.09, Hazard Ratio (HR) 0.4778, 95% CI from 0.2029 to 1.1253). **(B)** Kaplan–Meier curve for OS in our cohort of GBM patients stratified for low NEAT1 expression (<the median value) vs. high NEAT1 expression (>the median value). The last group was significantly associated to a worse outcome (n = 27, p = 0.035, HR 2.7980, 95% CI from 1.0754 to 7.2804). **(C)** Kaplan–Meier curve for OS in The Cancer Genome Atlas (TCGA) patients stratified for low miR-370-3p/ high NEAT1 vs. high miR-370-3p/ low NEAT1. The last group was significantly associated to a better outcome (n = 153, p = 0.0215, HR 0.6855, 95% CI from 0.4968 to 0.9458). **(D)** Kaplan–Meier curve for OS in GBM TCGA patients stratified for low miR-370-3p/high NEAT1/high HIF1A vs high miR-370-3p/low NEAT1/low HIF1A (n = 47, p = 0.4400, HR 0.7927, 95% CI from 0.4395 to 1.4296).

DISCUSSION

Thanks to advancements in genomics technology, the last years have seen an extensive exploration of the "dark matter" of the human genome, leading to the amazing discovery that it is far more extensively transcribed than was previously evaluated (Dykes and Emanueli, 2017). The role played by non-coding RNAs in regulating and influencing molecular and cellular processes cannot be underestimated, and their dysregulation is frequently related to several types of cancer (Mercer et al., 2009, Anastasiadou et al., 2018, Zhang et al., 2019b).
As a consequence, new studies aim to explore the potential role of miRNAs as biomarkers in the treatment of GBM, because their altered expression can affect glioma initiation and progression (Mizoguchi et al., 2012, Banelli et al., 2017). Diagnostic biomarkers allow a more precise classification of the tumor, prognostic biomarkers give more information about cancer outcomes, such as recurrence, progression and overall survival, and offer the possibility to tailor the treatment strategy improving therapeutic outcome minimising drug resistance, consequently facilitating patient management (Shergalis et al., 2018, DeOcesano-Pereira et al., 2020). The dysregulated expression of miRNAs within the DLK-DIO3 chromosomic region, like miR-370-3p, is correlated with tumor aggressiveness and clinical outcome of GBM patients, making it a primary research area (Benetatos et al., 2013, Shahar et al., 2016, Marziali et al., 2017).

Numerous studies have showed how the downregulation of miR-370-3p influences tumorigenicity in gliomas and especially in recurrent GBM (Gao et al., 2016). It has been demonstrated that unaltered expression of this miRNA may inhibit cell proliferation in glioma, acting as tumor suppressor while promoting apoptosis (Peng et al., 2016, Gong et al., 2018). Finally, the up-regulation of miR-370-3p seems to sensitise GBM cells to TMZ treatment (Gao et al., 2016).

In agreement with previous studies, our Real-Time Polymerase Chain Reaction (RT-PCR) results confirmed that miR-370-3p expression was significantly down-regulated in GBM tissues and in our collection of patient-derived GSC lines, when compared to the control normal brain tissues and normal NSCs. Our findings also reveal additional roles for miR-370-3p in GBM such as its involvement in cell growth, migration, and colony-forming ability of GSCs *in vitro*. Moreover, restoring the

expression of miR-370-3p decreased the growth of GSC-derived tumors *in vivo* and reduced its invasiveness (Figure 2, 3, and 4).

Furthermore, we investigated the regulatory network in which miR-370-3p could be involved, finding that it plays a tumor-suppressing function in GSCs by targeting the mRNAs coding for HMGA2 and HIF1A, genes involved in EMT and hypoxia. Hypoxia enhances the invasiveness of tumor cells by EMT, which worsens GBM aggressiveness, by the induction of a mesenchymal shift that is mediated by the HIF1A-ZEB1 axis, leading to an increased invasive potential (Joseph et al., 2015). HMGA2 is a member of the non-histone chromosomal high mobility group (HMG) protein family which mainly works as a regulating factor at transcriptional level by altering chromatin architecture and carrying out an important role in EMT in several tumors (Luo et al., 2013, Zha et al., 2013, Lu et al., 2018). Two of the main features of GBM are the intense cell proliferation and insufficient vascularization that leads to the presence of regions around the necrotic core of the tumor with insufficient oxygen supply (hypoxia) (Gaelzer et al., 2017). High spatially heterogeneity of GMB is also due to the niches created by hypoxia gradients (Hubert et al., 2016, Ou et al., 2020).

Intriguingly, among the most down-regulated genes in miR-370-3p-restored GSCs we found NT5E/CD73, a protein bound to the outer surface of the plasma membrane by a glycosylphosphatidylinositol (GPI) anchor, localised within lipid rafts (Zimmermann et al., 2012), acting as an ecto-5'-nucleotidase that hydrolyses extracellular adenosine monophosphate (AMP) into adenosine and inorganic phosphate (Robson et al., 2006). Moreover, CD73 has been found over-expressed in a variety of cancer cells and tumor patient biopsies, including gliomas, and it is associated with worse disease-free survival rates in GBM patients (Ludwig et al., 1999, Gao et al., 2014). CD73 is involved in the control of glioma cell migration and invasion through an adenosinergic pathway (Wang and Matosevic, 2019). The deregulation of CD73 impairs glioma cell migration and invasion by reducing metalloproteinase-2 and vimentin expression and reduced cell proliferation (Azambuja et al., 2019, Kitabatake et al., 2021). Those effects are also involved in the AKT/NF-kB pathway. Additionally, CD73 knockdown, or enzyme inhibition, potentiated TMZ cytotoxic effect on glioma (Azambuja et al., 2019). It is worth noting that HIF1A can directly bind to the NT5E promoter as well, activating its expression and confirming the role of NT5E in hypoxia adaptation even in GBM (Synnestvedt et al., 2002,

Colgan et al., 2006). Consequently, the hypoxic conditions, resulting from uncontrolled tumor cell proliferation, might induce the HIF1A-mediated up-regulation of NT5E expression on GSCs.

LncRNAs are extremely heterogeneous and have a considerable functional versatility that depends on their ability, as long RNA molecules, to conform to different structures and molecular interactions with proteins and nucleic acids, to modulate their activities temporally and spatially (Mercer et al., 2009, Marchese et al., 2017). Moreover, the deregulation of lncRNAs has been associated to cardiovascular and neurodegenerative diseases and cancers, including gliomas (Chen and Yan, 2013, Chi et al., 2019). LncRNAs and miRNAs can interact with each other and indeed, our analysis shows that this is possible also for miR-370-3p, as this microRNA binds directly the lncRNA NEAT1. The main function of NEAT1 is the nucleation of paraspeckles (specific nuclear structures) and is essential for their formation and maintenance (Clemson et al., 2009); moreover, NEAT1 controls 13.3% of genes in the PI3K-AKT signalling pathway by interacting with both promoter and distal regulatory elements, in a similar way as various other lncRNAs (Zhang et al., 2019a). NEAT1 is also found to act as an oncogene in most human cancers, including GBM (Zhen et al., 2016, Chen et al., 2018b). NEAT1 is also linked to, and induced by hypoxia: its induction promotes cell proliferation and inhibits apoptosis (Choudhry et al., 2015). Moreover, NEAT1 promotes EMT and correlates with a higher World Health Organization (WHO) grade assigned to human glioma tissue (Choudhry et al., 2015).

Our results have shown that NEAT1 expression levels are inversely correlated with miR-370-3p expression in our collection of GSCs and GBM tissues. It is known that NEAT1 over-expression in GBM correlates with clinic-pathological characteristics, such as larger tumor size, higher WHO grade, higher recurrence, and worse prognosis in glioma patients (He et al., 2016). In line with these clinical results, we found that over-expression of NEAT1 conferred malignancies to glioma, and our results confirms that NEAT1 knockdown in GSCs inhibited cell proliferation, invasion, and migration. Mechanistic studies proved that NEAT1 behaves as a competitive endogenous lncRNA sponging miR-449b-5p, inducing c-Met expression and thus potentially contributing to the development of glioma (Zhen et al., 2016). Further analyses found that NEAT1 expression levels in GBM are regulated by Epidermal Growth Factor Receptor (EGFR) pathway activity, which is mediated by STAT3 and NF-κB (p65) downstream of the EGFR pathway (Chen et al., 2018b).

Additionally, NEAT1 results critical for glioma cell growth and invasion, by increasing β-catenin nuclear transport and down-regulating ICAT, GSK3B, and Axin2, (Chen et al., 2018b).
Our results confirm the oncogenic role of NEAT1, the oncosuppressing role of miR-370-3p, and their interaction and inter-regulation in GBM; the use of patient-derived GSCs in this study also confirms their usefulness to obtain data that could be translated on different clinical settings thanks to their ability to mimic the original tumor (D'Alessandris et al., 2017).
These lncRNA–miRNA–mRNA cross-talks represent a key regulating factor in the maintenance of cellular homeostasis (Zhang et al., 2019b). The dysregulation of non-coding RNA (ncRNA) regulatory networks has already been described as having oncogenic or tumor-suppressive effects in many cancer types (Chan and Tay, 2018, Anastasiadou et al., 2018). In the same way, the lncRNA-miRNA co-expression network contributes to GBM onset, progression, angiogenesis, and drug resistance. Altogether, our results suggest a complex interplay among different species of RNAs in GSCs (Figure 12), in which miR-370-3p shows a prominent tumor-suppressor function by targeting mRNAs involved in EMT and in hypoxia pathways (i.e., HMGA2 and HIF1A, respectively). HIF1A, in turn, regulates transcription of NT5E/CD73, which are well-known to be involved in tumor development, in adaption to hypoxia and in promotion of immune-escape. Furthermore, the downregulation of miR-370-3p is associated with the over-expression of the lncRNA NEAT1, which enhances cell growth and invasiveness in GBM.
The importance of ncRNAs in a range of cancer types is well established and this makes them interesting therapeutic targets (Wang et al., 2019, Krichevsky and Uhlmann, 2019). Being RNA transcripts, the way to target them and manipulate their expression levels is by either altering the corresponding genomic DNA or by directly targeting the ncRNA molecules(Liu and Lim, 2018, Wang et al., 2019).
A possible strategy to modulate the expression of lncRNA NEAT1 could be the oligo-based therapy, which relies on synthetic oligonucleotides, such as ASOs (Antisense oligonucleotides) or siRNA (small interfering RNAs), to modulate the target expression (Roberts et al., 2020, Kim et al., 2018).
There is one principal obstacle in developing molecular therapies that target ncRNAs in brain tumors such as GBM: the presence of the blood-brain barrier (BBB), a complex structure that primarily prevents hydrophilic agents from accessing the brain(Pottoo et al., 2021, Krichevsky and Uhlmann, 2019).

The presence of the BBB blocks traditional delivery methods for medicaments; malignant brain tumors can cause partial disruptions to this barrier, but it is not enough to make the tumor site more accessible(Krichevsky and Uhlmann, 2019). Different approaches have been proposed to overcome this obstacle, such as the repeated BBB opening through ultrasound to facilitate drug delivery and chemotherapy (Krichevsky and Uhlmann, 2019). Moreover, medicaments that use ncRNAs have high susceptibility to degradation and therefore can be eliminated before reaching their target site (Krichevsky and Uhlmann, 2019, Javed et al., 2018)

A different strategy could be offered by the development of nanoparticles, optimised for targeted drug delivery of biological macromolecules (such as peptides, RNA, and miRNAs); the macromolecule is thus protected from degradation and can more easily enter the BBB to target dysregulated ncRNAs (Pottoo et al., 2021, Krichevsky and Uhlmann, 2019, Kim et al., 2018).

A deeper understanding of the complex networks of interactions coordinated by ncRNAs is needed to improve our knowledge of a complex tumor such as GBM. Furthermore, the comprehension of the lncRNA–miRNA–mRNA interplay could unveil novel applications of ncRNAs not only as diagnostic and predictive biomarkers, but also as targets of cancer therapy itself, informing the development of precision medicine and leading to new combination therapies as promising methods for GBM treatment.

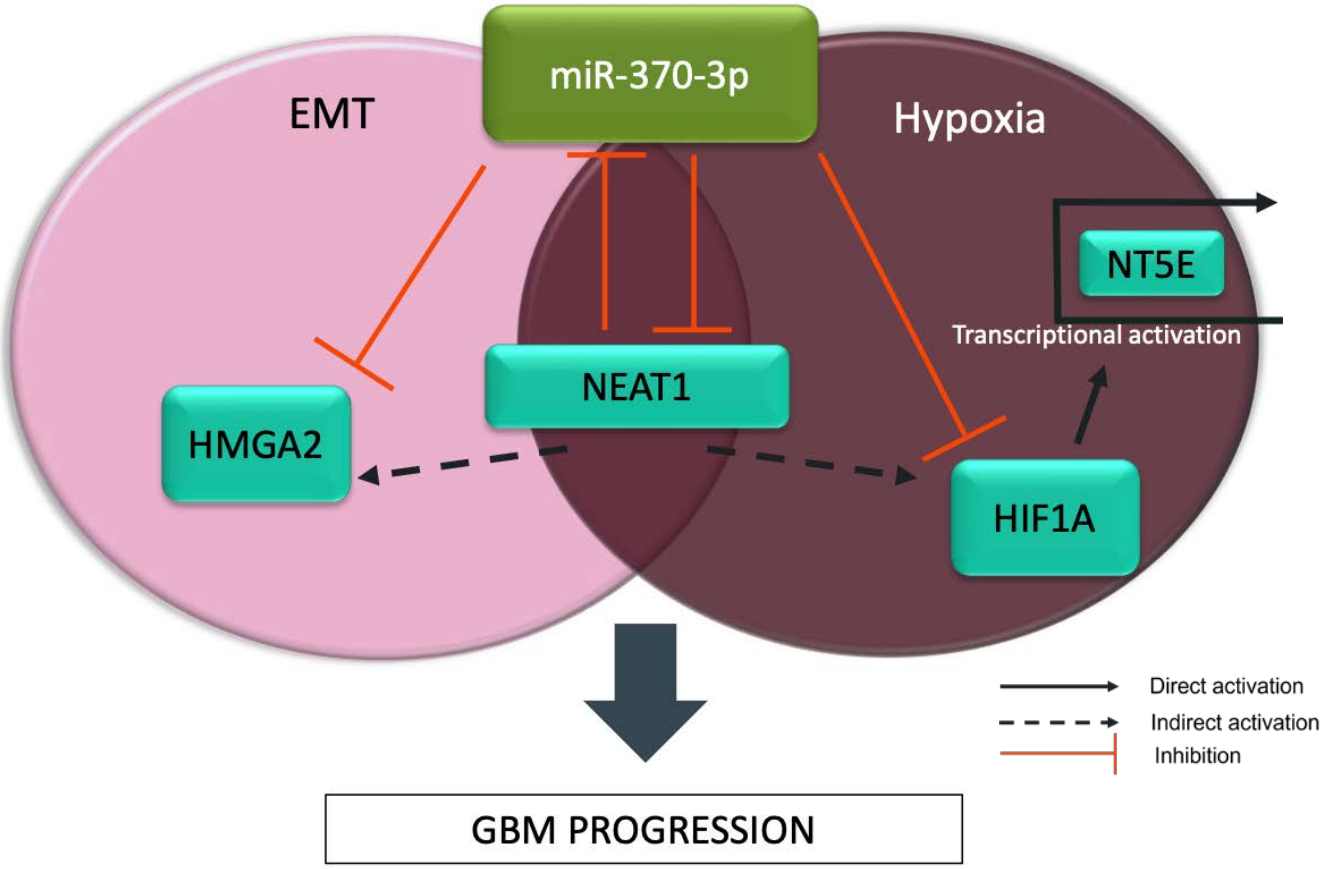

Figure 12 Schematic drawing of the reciprocal regulation/interaction between miR-370-3p and NEAT1 and their impact on the HMGA2-HIF1A-NT5E interplay.

STAR METHODS
KEY RESOURCES TABLE

REAGENT OR RESOURCE	SOURCE	IDENTIFIER
Biological Samples		
Glioblastoma tissues	Institute of Neurosurgery, Catholic University School of Medicine in Rome	N/A
Normal brain tissues	Institute of Neurosurgery, Catholic University School of Medicine in Rome	N/A
Antibodies		
Anti-Human Ki-67	Dako	Cat#F7268
Brilliant Violet 421™ anti-human CD73	BioLegend	Cat#344007
BV421 Mouse IgG1, k Isotype Control	BD Biosciences	Cat# AB_11207319
Chemicals, Peptides and Recombinant proteins		
TRIzol™ Reagent	Life Technologies Corporation	Cat#15596
M-MLV Reverse Transcriptase	Invitrogen	Cat# 28025013
Calcium phosphate	Sigma Aldrich	Cat# 16483
HBSS	N/A	N/A
Calcein-AM	Life Technologies Corporation	C1430
Doxycycline	Sigma Aldrich	D9891
Lipofectamine 2000	Invitrogen	Cat#11668019
Hoechst 33342	Sigma Aldrich	Cat#62249

Eukitt	EMS	Cat#15320
Critical Commercial Assays		
TaqMan™ MicroRNA Reverse Transcription Kit	Applied Biosystems	Cat# 4366596
Cell ID. System	Promega	B9510
TaqMan™ MicroRNA Reverse Transcription Kit	Applied Biosystems	Cat# 4366596
TaqMan™ MicroRNA Assay ID 002275	Applied Biosystems	Cat# 4427975
TaqMan™ MicroRNA Assay ID: 001093	Applied Biosystems	Cat#4427975
SYBR™ Green PCR Master Mix	Applied Biosystems	Cat# 4309155
CellTiter-Blue Viability Assay	Promega	G8080
Affymetrix GeneChip1.0 ST array	Affymetrix, Santa Clara	N/A
Dual Luciferase Reporter kit	Promega Inc.	E1910
Experimental Models: Cell Lines		
Patient-derived GSCs	Institute of Neurosurgery Catholic University Pallini *et al.,* 2008	N/A
HNPCs	Lonza	Cat# PT-2599
HEK293T	ATCC	CRL-3216
Experimental Models: Organisms/strains		
NOD/SCID mice	Charles River, Italy	N/A
Oligonucleotides		
Pri-miRNA-370-3p amplification primers: For-5'-CTACTCGAGGGATGGGCGATAGTTCAGGT-3' Rev-5'-TATGCGGCCGCGCCCGAGCTCTGGTGTTA-3'	N/A	N/A

HIF1A primers: For-5'-CATCAGCTATTTGCGTGTGAGGA-3' Rev-5'-AGCAATTCATCTGTGCTTTCATGTC-3'	N/A	N/A
HMGA2 primers: For- 5'-AGTCCCTCTAAAGCAGCTCA-3' Rev-5'- GTCCTCTTCGGCAGACTCTT-3'	N/A	N/A
NEAT1 primers: For-5'-TGCTTGTTCCAGAGCCCATGAATGCCA-3' Rev-5'-GTTCTACAGCTTAGGGATCTTCTTGAAGC-3'		
GAPDH primers: For-5'-ACCTGACCTGCCGTCTAGAAAA-3' Rev-5'-CCTGCTTCACCACCTTCTTGA-3'	N/A	N/A
Recombinant DNA		
TRIPZ doxycycline inducible lentiviral vector	Thermofisher Scientific	N/A
psiCHECK(TM)-2 control Vector	Promega Inc.	N/A
Software and Algorithms		
GraphPad Prism v4.0	GraphPad Software	www.graphpad.com
Gene Set Enrichment Analysis (GSEA) software		www.gsea-msigdb.org/gsea/index.jsp
TargetScan		www.targetscan.org
miRanda		www.microrna.org
starBase v2.0		starbase.sysu.edu.cn

EXPERIMENTAL MODEL AND SUBJECT DETAILS

Patients and tumor samples

All human GBM and normal brain tissues were collected from adult patients who underwent surgery for complete or partial resection of GBM or craniotomy for non-tumoral pathology, at the Institute of Neurosurgery, Catholic University School of Medicine in Rome. All the patients provided written informed consent according to the research proposals approved by the Ethical Committee of the Catholic University School of Medicine (no. 1720). A diagnosis of GBM was established histologically by the neuropathologist in accordance with the WHO classification (Louis et al., 2016).

Glioblastoma stem-like cells were isolated from surgical samples subjected to mechanical dissociation and the resulting cell suspension was cultured in a Dulbecco's modified Eagle's medium/F12 serum free medium containing 0.6% glucose, 9.6 g/mL putrescine, 2 mM glutamine, 6.3 ng/mL progesterone, 5.2 ng/mL sodium selenite, 0.025 mg/mL insulin, and 0.1 mg/mL transferrin sodium salt supplemented with 20 ng/ml epidermal growth factor (EGF) and 10 ng/ml basic fibroblast growth factor (b-FGF). Cells were cultured for 3 to 4 weeks, until they established and grew as spheroids.

Cell Lines

GSC lines were validated by Short Tandem Repeat (STR) DNA fingerprinting. Nine highly polymorphic STR loci plus amelogenin (Cell ID. System, Promega Inc., Madison, WI) were used. Detection of amplified fragments was obtained by ABI PRISM 3100 Genetic Analyzer (Applied Biosystems, Carlsbad, CA, USA). Data analysis was performed by GeneMapper® software, version 4.0 (Biological Bank and Cell Factory, National Institute for Cancer Research, IST, Genoa, Italy). All GSC profiles were challenged against public databases to confirm authenticity. Human adult neural stem cell line was isolated from human neural adult tissue obtained following the ethical guidelines of the NECTAR and the Declaration of Helsinki from patients undergoing particularly invasive neurosurgery as previously described (Ricci-Vitiani *et al.,* 2004). Human neural stem cell (HNSC) lines were purchased from Lonza (Lonza Inc.,Walkersville,

MD, USA). Packaging cell line, 293T, was maintained in DMEM (Life Technologies Corporation, Carlsbad, CA, USA) supplemented with 10%

(v/v) heat-inactivated FBS, 2mML-glutamine, 100 U/mL of penicillin and 100 mg/mL of streptomycin (Invitrogen, Carlsbad, CA, USA).

Animal models

Animal experiments were performed in accordance with relevant institutional and national regulations.

METHOD DETAILS

Real-Time PCR

Total RNA was extracted from cells using TRIzol reagent (Life Technologies Corporation) and reverse transcribed by Moloney Murine Leukemia Virus enzyme (M-MLV) with random primers (Invitrogen). Analysis of mature miR-370-3p was performed using TaqMan® miRNA Assay protocol (assay ID 002275, Applied Biosystems) and normalized with RNU6B (Assay ID: 001093, Applied Biosystems).

Real-time PCR for HMGA2, HIF1A, and NEAT1 mRNA detection were performed with SYBR™ Green Master Mix in StepOnePlus (Applied Biosystems) and samples normalized in respect to GAPDH. All RT-PCR reactions were run in duplicate in StepOne Real-Time PCR System (Applied Biosystems, Foster City, CA, USA).

List of primers used below:

HIF1A 5′-CATCAGCTATTTGCGTGTGAGGA-3′ (Forward)

5′-AGCAATTCATCTGTGCTTTCATGTC-3′ (Reverse)

HMGA2 5′-AGTCCCTCTAAAGCAGCTCA-3′ (Forward)

5′- GTCCTCTTCGGCAGACTCTT-3′ (Reverse)

NEAT1 5′-TGCTTGTTCCAGAGCCCATGAATGCCA-3′ (Forward)

5′-GTTCTACAGCTTAGGGATCTTCTTGAAGC-3′ (Reverse)

GAPDH 5′-ACCTGACCTGCCGTCTAGAAAA-3′ (Forward)

5′-CCTGCTTCACCACCTTCTTGA-3′ (Reverse)

Plasmid Constructs and Lentivirus Infection

To restore the expression of miR-370-3p in GSCs, we cloned its precursor in the 30-untranslated (UTR) region of RFP in the TRIPZ doxycycline inducible lentiviral vector (ThermoFisher Scientific,Waltham, MA, USA). Primers used for pri-miRNA-370 amplification were:

5′-CTACTCGAGGGATGGGCGATAGTTCAGGT-3′(Forward)

5′-TATGCGGCCGCGCCCGAGCTCTGGTGTTA-3′ (Reverse).

The short hairpin (sh)RNA sequence targeting NEAT1 (50-gatccctaagctgtagaacat-30, DOI: 10.1002/jcp.27093) was synthesized and cloned in GFP-C-shLenti-vector from OriGene (OriGene Technologies, Inc., Rockville, MD, USA).

Lentiviral particles were produced by the calcium phosphate transfection protocol in 293T packaging cell line and infection performed as previously described (Ricci-Vitiani et al., 2004). Briefly, 20 μg of lentiviral vector was co-transfected with 13 μg of pMD2G (Addgene, USA;12259) and 7 μg of psPAX2 (Addgene, USA; 12260). The calcium-phosphate DNA precipitate was removed after 6-7h by replacing the medium. Viral supernatant was collected 36h post-transfection, filtered through a 0.45 μm-pore size filter and added to GSCs in the presence of 4 μg/ml polybrene. GSCs were centrifuged for 30 minutes at 1800 rpm. After infection for TRIPZ and TRIPZ-miR-370 vectors, transduced cells were selected with puromycin, and Red Fluorescent Protein (RFP) fluorescence was evaluated by FACSCanto (BD Biosciences) upon doxycycline induction (2μg/ml) (Sigma Aldrich Inc., Saint Louis, MO).

About shNTC and shNEAT vectors, Green Fluorescent Protein (GFP) fluorescence of transduced cells was evaluated by FACSCanto (BD Biosciences) and GFP-positive cells were flow sorted by FACS ARIA (BD Biosciences).

Cell Growth, Migration, and Colony Formation Assay

For the viability assay TRIPZ and TRIPZ-miR-370 GSCs were plated at density of 2 x 10^4/mL in 96-well plates in triplicate. Cell viability was monitored by counting the cells and confirmed by using the CellTiter-

Blue Viability Assay (Promega): we added 20 µl of the CellTiter-Blue® Reagent directly to each well, then we incubated the plates for 1 hour at 37°C to allow viable cells to reduce the indicator dye resazurin into the highly fluorescent resorufin. After the reaction we measured the fluorescent signal by MultiLabel Plate Reader VICTOR X3™ (Perkin Elmer, USA). The same procedure was applied to GSCs transduced with the short hairpin (sh)RNA sequence targeting NEAT1 and GSCs transduced with shNTC (Non Target Control) sequence as a control.

We tested the migration and invasion capability of transduced GSCs by plating them in Corning FluoroBlok Multiwell Inserts System (Corning Life Sciences, Tewksbury, MA, USA), according to manufacturer's instruction. We plated 3x 10^4 cells in the upper chamber in stem cell medium without growth factors. Stem cell medium supplemented with growth factors (EGF and bFGF) was added in the lower chamber and used as chemoattractant. After 48h, we added the fluorescent dye calcein acetoxymethyl ester (calcein-AM, Life Technologies Corporation) to the lower chamber and incubated the plate for 30 min at 37 °C. The cell viability indicator, calcein-AM, is a non-fluorescent, cell permeate compound that is hydrolyzed by intracellular esterases into the fluorescent anion calcein and can be used to fluorescently label viable cells before microscope observation. After imaging acquisition using a fluorescence microscope, we counted the number of migrated cells.

We evaluated the colony formation ability of transduced GSCs by plating a single cell/well in 96-well plates. After 3-4 weeks, we examined each well, and we counted the number of spheres/cell aggregates. All the experiments were performed in stem cell medium, previously described in the cell culture section, in the presence of doxycycline.

Orthotopic Xenograft Mouse Models

For the animal experiments, 2 x10^5 TRIPZ and TRIPZ-miR-370 GSCs were intracranially injected into NOD/SCID mice (*n*, 6; 4–6 weeks of age; CD1 NOD-/SCID mice, Charles River, Italy). Before grafting, mice were anesthetized with intraperitoneal injection of diazepam (2 mg/100 g) followed by intramuscular injection of ketamine (4 mg/100 g). The animal skulls were immobilized in a stereotactic head frame and a burr hole were made 2 mm right of the midline and 1 mm posterior to the coronal suture. The tip of a 10 µl Hamilton micro-syringe was placed at a depth of 3 mm from the dura and the cells were slowly injected.

Doxycycline administration in drinking water (200 μg/mL) started the day of injection. After 4 weeks of survival, mice were deeply anesthetized and transcardially perfused with 0.1 M PBS (pH = 7.4), followed by 4% paraformaldehyde in 0.1 M PBS. The brain was removed, stored in 30% sucrose buffer overnight at 4 °C and serially cut by cryostat at 20 μm on the coronal plane. Sections were collected in distilled water, mounted on slides, and cover-slipped with Eukitt. Images were acquired with a Laser Scanning Confocal Microscope (IX81, Olympus Inc., Melville, NY, USA). Tumor volumes were calculated on histological section through the tumor epicenter, according to the Equation (1),

$$V = (a^2 \times b)/2$$

where a is the shortest diameter and b is the longest diameter of tumors.

Immunofluorescence was performed as previously described (Mollinari et al., 2009). Briefly, utilizing antiserum directed against Ki67 (Dako, Glostrup, Denmark). To calculate the percentage of antigen-expressing tumor cells, at least 1000 cells were counted across 10 different fields.

Noncoding-RNA Target Prediction

TargetScan (http://www.targetscan.org), miRanda (http://www.microrna.org), starBase v2.0 (http://starbase.sysu.edu.cn) were used for miR-370-3p target prediction.

Luciferase assay

The human HIF1A 3′-UTR and NEAT1 sequences containing the target sites for miR-370-3p were amplified by PCR from genomic DNA and cloned into pGL3 control vector or psiCHECK(TM)-2 Vector (Promega Inc.) downstream of the luciferase reporter gene. The mutant plasmid containing mutations of the miR-370-3p target sites were obtained by site-specific mutagenesis. Plasmids were verified by sequence analysis. Human 293T cells were transiently co-transfected by Lipofectamine 2000 (Invitrogen), with 400 ng of luciferase reporter plasmid containing wild-type or mutated HIF1A 3′-UTR-seed sequence or mutated NEAT1seed sequence for miR-370-3p, 10 pmol of either the hsa-miR370-3p mimic or control-mimic oligonucleotides (Ambion, Life technologies). Thirty-six

hours post-transfection luciferase activity was quantified by Dual Luciferase Reporter kit (Promega Inc.).

Flow Cytometry

For CD73 expression, TRIPZ and TRIPZ-miR-370 GSCs were incubated with the antibody for 30 min at RT, washed with PBS and analyzed by CytoFLEX LX flow cytometer (Beckman Coulter, Brea, CA, USA) equipped with a CytExpert software (Beckman Coulter Life Science, Milan, Italy). The antibody used was Brilliant Violet (BV) 421-conjugated mouse anti-human CD73/NT5E antibody or BV421-conjugated mouse IgG1 isotype control antibody (BD Biosciences, Milan, Italy). The staining was performed after doxycycline induction.

Gene array

To analyze whether miR-370-3p restoration affects gene expression patterns in GSCs, we performed a gene array as previously described (Marziali et al., 2017). Total RNA was extracted from TRIPZ and TRIPZ-miR-370 GSC#1 stably transduced cells. RNA was labeled and hybridized to the Affymetrix GeneChip1.0 ST array (Affymetrix, Santa Clara, CA, USA) following the manufacturer's instructions. Hybridization values were normalized by the RMA method, and transcripts displaying differential expression were selected when the fold modulation exceeded the value of 2.

QUANTIFICATION AND STATISTICAL ANALYSIS

Statistical analysis was performed by means of GraphPad prism v4.0 (GraphPad Software, La Jolla, CA, USA, www.graphpad.com). Statistical significance reported on the plots is the following: * $p < 0.05$, ** $p < 0.01$ and *** $p < 0.001$.

REFERENCES

AHMED, A. U., AUFFINGER, B. & LESNIAK, M. S. 2013. Understanding glioma stem cells: rationale, clinical relevance and therapeutic strategies. *Expert Rev Neurother,* 13**,** 545-55.

ALDAZ, B., SAGARDOY, A., NOGUEIRA, L., GURUCEAGA, E., GRANDE, L., HUSE, J. T., AZNAR, M. A., DÍEZ-VALLE, R., TEJADA-SOLÍS, S. & ALONSO, M. M. 2013. Involvement of miRNAs in the differentiation of human glioblastoma multiforme stem-like cells. *PloS one,* 8**,** e77098.

ANASTASIADOU, E., JACOB, L. S. & SLACK, F. J. 2018. Non-coding RNA networks in cancer. *Nat Rev Cancer,* 18**,** 5-18.

AZAMBUJA, J. H., GELSLEICHTER, N. E., BECKENKAMP, L. R., ISER, I. C., FERNANDES, M. C., FIGUEIRO, F., BATTASTINI, A. M. O., SCHOLL, J. N., DE OLIVEIRA, F. H., SPANEVELLO, R. M., SEVIGNY, J., WINK, M. R., STEFANI, M. A., TEIXEIRA, H. F. & BRAGANHOL, E. 2019. CD73 Downregulation Decreases In Vitro and In Vivo Glioblastoma Growth. *Mol Neurobiol,* 56**,** 3260-3279.

BALLANTYNE, M. D., MCDONALD, R. A. & BAKER, A. H. 2016. lncRNA/MicroRNA interactions in the vasculature. *Clin Pharmacol Ther,* 99**,** 494-501.

BANAN, R. & HARTMANN, C. 2017. The new WHO 2016 classification of brain tumors-what neurosurgeons need to know. *Acta Neurochir (Wien),* 159**,** 403-418.

BANELLI, B., FORLANI, A., ALLEMANNI, G., MORABITO, A., PISTILLO, M. P. & ROMANI, M. 2017. MicroRNA in glioblastoma: an overview. *International journal of genomics,* 2017.

BARONCHELLI, S., BENTIVEGNA, A., REDAELLI, S., RIVA, G., BUTTA, V., PAOLETTA, L., ISIMBALDI, G., MIOZZO, M., TABANO, S., DAGA, A., MARUBBI, D., CATTANEO, M., BIUNNO, I. & DALPRA, L. 2013. Delineating the cytogenomic and epigenomic landscapes of glioma stem cell lines. *PLoS One,* 8**,** e57462.

BARTEL, D. P. 2009. MicroRNAs: target recognition and regulatory functions. *Cell,* 136**,** 215-33.

BARTONICEK, N., MAAG, J. L. & DINGER, M. E. 2016. Long noncoding RNAs in cancer: mechanisms of action and technological advancements. *Mol Cancer,* 15**,** 43.

BENETATOS, L., HATZIMICHAEL, E., LONDIN, E., VARTHOLOMATOS, G., LOHER, P., RIGOUTSOS, I. & BRIASOULIS, E. 2013. The microRNAs within the DLK1-DIO3 genomic region: involvement in disease pathogenesis. *Cell Mol Life Sci,* 70**,** 795-814.

BHAN, A., SOLEIMANI, M. & MANDAL, S. S. 2017. Long Noncoding RNA and Cancer: A New Paradigm. *Cancer Res,* 77**,** 3965-3981.

CAI, F., DAI, C., CHEN, S., WU, Q., LIU, X., HONG, Y., WANG, Z., LI, L., YAN, W., WANG, R. & ZHANG, J. 2019. CXCL12-regulated miR-370-3p functions as a tumor suppressor gene by targeting HMGA2 in nonfunctional pituitary adenomas. *Mol Cell Endocrinol,* 488**,** 25-35.

CAO, X., LIU, D., YAN, X., ZHANG, Y., YUAN, L., ZHANG, T., FU, M., ZHOU, Y. & WANG, J. 2013. Stat3 inhibits WTX expression through up-regulation of microRNA-370 in Wilms tumor. *FEBS Lett,* 587**,** 639-44.

CHAN, J. A., KRICHEVSKY, A. M. & KOSIK, K. S. 2005. MicroRNA-21 is an antiapoptotic factor in human glioblastoma cells. *Cancer research,* 65**,** 6029-6033.

CHAN, J. J. & TAY, Y. 2018. Noncoding RNA:RNA Regulatory Networks in Cancer. *Int J Mol Sci,* 19.

CHANG, K. W., CHU, T. H., GONG, N. R., CHIANG, W. F., YANG, C. C., LIU, C. J., WU, C. H. & LIN, S. C. 2013. miR-370 modulates insulin receptor substrate-1 expression and inhibits the tumor phenotypes of oral carcinoma. *Oral Dis,* 19**,** 611-9.

CHEN, F., FENG, Z., ZHU, J., LIU, P., YANG, C., HUANG, R. & DENG, Z. 2018a. Emerging roles of circRNA_NEK6 targeting miR-370-3p in the proliferation and invasion of thyroid cancer via Wnt signaling pathway. *Cancer biology & therapy,* 19**,** 1139-1152.

CHEN, J., LIU, G., WU, Y., MA, J., WU, H., XIE, Z., CHEN, S., YANG, Y., WANG, S. & SHEN, P. 2019. CircMYO10 promotes osteosarcoma progression by regulating miR-370-3p/RUVBL1 axis to enhance the transcriptional activity of β-catenin/LEF1 complex via effects on chromatin remodeling. *Molecular cancer,* 18**,** 1-24.

CHEN, Q., CAI, J., WANG, Q., WANG, Y., LIU, M., YANG, J., ZHOU, J., KANG, C., LI, M. & JIANG, C. 2018b. Long Noncoding RNA NEAT1, Regulated by the EGFR Pathway, Contributes to Glioblastoma Progression Through the WNT/beta-Catenin Pathway by Scaffolding EZH2. *Clin Cancer Res,* 24**,** 684-695.

CHEN, X. & YAN, G.-Y. 2013. Novel human lncRNA–disease association inference based on lncRNA expression profiles. *Bioinformatics,* 29**,** 2617-2624.

CHEN, X. P., CHEN, Y. G., LAN, J. Y. & SHEN, Z. J. 2014. MicroRNA-370 suppresses proliferation and promotes endometrioid ovarian cancer chemosensitivity to cDDP by negatively regulating ENG. *Cancer Lett,* 353**,** 201-10.

CHI, Y., WANG, D., WANG, J., YU, W. & YANG, J. 2019. Long Non-Coding RNA in the Pathogenesis of Cancers. *Cells,* 8.

CHOUDHRY, H., ALBUKHARI, A., MOROTTI, M., HAIDER, S., MORALLI, D., SMYTHIES, J., SCHODEL, J., GREEN, C. M., CAMPS, C., BUFFA, F., RATCLIFFE, P., RAGOUSSIS, J., HARRIS, A. L. & MOLE, D. R. 2015. Tumor hypoxia induces nuclear paraspeckle formation through HIF-2alpha dependent transcriptional activation of NEAT1 leading to cancer cell survival. *Oncogene,* 34**,** 4482-90.

CLEMSON, C. M., HUTCHINSON, J. N., SARA, S. A., ENSMINGER, A. W., FOX, A. H., CHESS, A. & LAWRENCE, J. B. 2009. An architectural role for a nuclear noncoding RNA: NEAT1 RNA is essential for the structure of paraspeckles. *Molecular cell,* 33**,** 717-726.

COLGAN, S. P., ELTZSCHIG, H. K., ECKLE, T. & THOMPSON, L. F. 2006. Physiological roles for ecto-5'-nucleotidase (CD73). *Purinergic Signal,* 2**,** 351-60.

D'ALESSANDRIS, Q. G., BIFFONI, M., MARTINI, M., RUNCI, D., BUCCARELLI, M., CENCI, T., SIGNORE, M., STANCATO, L., OLIVI, A., DE MARIA, R., LAROCCA, L. M., RICCI-VITIANI, L. & PALLINI, R. 2017. The clinical value of patient-derived glioblastoma tumorspheres in predicting treatment response. *Neuro Oncol,* 19**,** 1097-1108.

DEOCESANO-PEREIRA, C., MACHADO, R. A., CHUDZINSKI-TAVASSI, A. M. & SOGAYAR, M. C. 2020. Emerging roles and potential applications of non-coding RNAs in glioblastoma. *International Journal of Molecular Sciences,* 21**,** 2611.

DONG, H., LEI, J., DING, L., WEN, Y., JU, H. & ZHANG, X. 2013. MicroRNA: function, detection, and bioanalysis. *Chemical reviews,* 113**,** 6207-6233.

DYKES, I. M. & EMANUELI, C. 2017. Transcriptional and Post-transcriptional Gene Regulation by Long Non-coding RNA. *Genomics Proteomics Bioinformatics,* 15**,** 177-186.

ENGREITZ, J. M., HAINES, J. E., PEREZ, E. M., MUNSON, G., CHEN, J., KANE, M., MCDONEL, P. E., GUTTMAN, M. & LANDER, E. S. 2016. Local regulation of gene expression by lncRNA promoters, transcription and splicing. *Nature,* 539**,** 452-455.

ERNST, A., HOFMANN, S., AHMADI, R., BECKER, N., KORSHUNOV, A., ENGEL, F., HARTMANN, C., FELSBERG, J., SABEL, M., PETERZIEL, H., DURCHDEWALD, M., HESS, J., BARBUS, S., CAMPOS, B., STARZINSKI-POWITZ, A., UNTERBERG, A., REIFENBERGER, G., LICHTER, P., HEROLD-MENDE, C. & RADLWIMMER, B. 2009. Genomic and expression profiling of glioblastoma stem cell-like spheroid cultures identifies novel tumor-relevant genes associated with survival. *Clin Cancer Res,* 15**,** 6541-50.

ESTELLER, M. J. N. R. G. 2011. Non-coding RNAs in human disease. 12**,** 861-874.

FERRIS, S. P., HOFMANN, J. W., SOLOMON, D. A. & PERRY, A. 2017. Characterization of gliomas: from morphology to molecules. *Virchows Arch,* 471**,** 257-269.

GAELZER, M. M., SANTOS, M. S. D., COELHO, B. P., DE QUADROS, A. H., SIMAO, F., USACH, V., GUMA, F. C. R., SETTON-AVRUJ, P., LENZ, G. & SALBEGO, C. G. 2017. Hypoxic and Reoxygenated Microenvironment: Stemness and Differentiation State in Glioblastoma. *Mol Neurobiol,* 54**,** 6261-6272.

GAO, Y. T., CHEN, X. B. & LIU, H. L. 2016. Up-regulation of miR-370-3p restores glioblastoma multiforme sensitivity to temozolomide by influencing MGMT expression. *Sci Rep,* 6**,** 32972.

GAO, Z.-W., DONG, K. & ZHANG, H.-Z. 2014. The roles of CD73 in cancer. *BioMed research international,* 2014.

GIMPLE, R. C., BHARGAVA, S., DIXIT, D. & RICH, J. N. 2019. Glioblastoma stem cells: lessons from the tumor hierarchy in a lethal cancer. *Genes Dev,* 33**,** 591-609.

GONG, L., XU, H., CHANG, H., TONG, Y., ZHANG, T. & GUO, G. 2018. Knockdown of long non-coding RNA MEG3 protects H9c2 cells from hypoxia-induced injury by targeting microRNA-183. *J Cell Biochem,* 119**,** 1429-1440.

HE, C., JIANG, B., MA, J. & LI, Q. 2016. Aberrant NEAT1 expression is associated with clinical outcome in high grade glioma patients. *APMIS,* 124**,** 169-74.

HILL, M. & TRAN, N. 2021. miRNA interplay: Mechanisms and consequences in cancer. *Disease Models & Mechanisms,* 14**,** dmm047662.

HUBERT, C. G., RIVERA, M., SPANGLER, L. C., WU, Q., MACK, S. C., PRAGER, B. C., COUCE, M., MCLENDON, R. E., SLOAN, A. E. & RICH, J. N. 2016. A Three-Dimensional Organoid Culture System Derived from Human Glioblastomas Recapitulates the Hypoxic Gradients and Cancer Stem Cell Heterogeneity of Tumors Found In VivoBrain Cancer Stem Cell Organoids. *Cancer research,* 76**,** 2465-2477.

JANJUA, T. I., REWATKAR, P., AHMED-COX, A., SAEED, I., MANSFELD, F. M., KULSHRESHTHA, R., KUMERIA, T., ZIEGLER, D. S., KAVALLARIS, M., MAZZIERI, R. & POPAT, A. 2021. Frontiers in the treatment of glioblastoma: Past, present and emerging. *Adv Drug Deliv Rev,* 171**,** 108-138.

JAVED, M. N., KOHLI, K. & AMIN, S. J. A. P. 2018. Risk assessment integrated QbD approach for development of optimized bicontinuous mucoadhesive limicubes for oral delivery of rosuvastatin. 19**,** 1377-1391.

KIM, S.-S., HARFORD, J. B., MOGHE, M., RAIT, A., PIROLLO, K. F. & CHANG, E. H. J. N. A. R. 2018. Targeted nanocomplex carrying siRNA against MALAT1 sensitizes glioblastoma to temozolomide. 46**,** 1424-1440.

KITABATAKE, K., KAJI, T. & TSUKIMOTO, M. 2021. Involvement of CD73 and A2B receptor in radiation-induced DNA damage response and cell migration in human glioblastoma A172 cells. *Biological and Pharmaceutical Bulletin,* 44**,** 197-210.

KONG, X., ZHAO, Y., LI, X., TAO, Z., HOU, M. & MA, H. 2019. Overexpression of HIF-2alpha-Dependent NEAT1 Promotes the Progression of Non-Small Cell Lung Cancer through miR-101-3p/SOX9/Wnt/beta-Catenin Signal Pathway. *Cell Physiol Biochem,* 52**,** 368-381.

KRICHEVSKY, A. M. & UHLMANN, E. J. J. N. 2019. Oligonucleotide therapeutics as a new class of drugs for malignant brain tumors: targeting mRNAs, regulatory RNAs, mutations, combinations, and beyond. 16**,** 319-347.

LEE, J., KOTLIAROVA, S., KOTLIAROV, Y., LI, A., SU, Q., DONIN, N. M., PASTORINO, S., PUROW, B. W., CHRISTOPHER, N., ZHANG, W., PARK, J. K. & FINE, H. A. 2006. Tumor stem cells derived from glioblastomas cultured in bFGF and EGF more closely mirror the phenotype and genotype of primary tumors than do serum-cultured cell lines. *Cancer Cell,* 9**,** 391-403.

LI, J. H., LIU, S., ZHOU, H., QU, L. H. & YANG, J. H. 2014. starBase v2.0: decoding miRNA-ceRNA, miRNA-ncRNA and protein-RNA interaction networks from large-scale CLIP-Seq data. *Nucleic Acids Res,* 42**,** D92-7.

LIU, B., PANG, B., HOU, X., FAN, H., LIANG, N., ZHENG, S., FENG, B., LIU, W., GUO, H., XU, S. & PANG, Q. 2014. Expression of high-mobility group AT-hook protein 2 and its prognostic significance in malignant gliomas. *Hum Pathol,* 45**,** 1752-8.

LIU, S. J. & LIM, D. A. J. E. R. 2018. Modulating the expression of long non-coding RNA s for functional studies. 19**,** e46955.

LO, S. S., HUNG, P. S., CHEN, J. H., TU, H. F., FANG, W. L., CHEN, C. Y., CHEN, W. T., GONG, N. R. & WU, C. W. 2012. Overexpression of miR-370 and downregulation of its novel target TGFbeta-RII contribute to the progression of gastric carcinoma. *Oncogene,* 31**,** 226-37.

LU, M., WANG, Y., ZHOU, S., XU, J., LI, J., TAO, R. & ZHU, Y. 2018. MicroRNA-370 suppresses the progression and proliferation of human astrocytoma and glioblastoma by negatively regulating beta-catenin and causing activation of FOXO3a. *Exp Ther Med,* 15**,** 1093-1098.

LUDWIG, H. C., RAUSCH, S., SCHALLOCK, K. & MARKAKIS, E. 1999. Expression of CD 73 (ecto-5'-nucleotidase) in 165 glioblastomas by immunohistochemistry and electronmicroscopic histochemistry. *Anticancer Res,* 19**,** 1747-52.

LUO, Y., LI, W. & LIAO, H. 2013. HMGA2 induces epithelial-to-mesenchymal transition in human hepatocellular carcinoma cells. *Oncol Lett,* 5**,** 1353-1356.

MAHINFAR, P., BARADARAN, B., DAVOUDIAN, S., VAHIDIAN, F., CHO, W. C.-S. & MANSOORI, B. 2021. Long non-coding RNAs in multidrug resistance of glioblastoma. *Genes,* 12**,** 455.

MARCHESE, F. P., RAIMONDI, I. & HUARTE, M. 2017. The multidimensional mechanisms of long noncoding RNA function. *Genome biology,* 18**,** 1-13.

MARZIALI, G., BUCCARELLI, M., GIULIANI, A., ILARI, R., GRANDE, S., PALMA, A., D'ALESSANDRIS, Q. G., MARTINI, M., BIFFONI, M., PALLINI, R. & RICCI-VITIANI, L. 2017. A three-microRNA signature identifies two subtypes of glioblastoma patients with different clinical outcomes. *Mol Oncol,* 11**,** 1115-1129.

MARZIALI, G., SIGNORE, M., BUCCARELLI, M., GRANDE, S., PALMA, A., BIFFONI, M., ROSI, A., D'ALESSANDRIS, Q. G., MARTINI, M., LAROCCA, L. M., DE MARIA, R., PALLINI, R. & RICCI-VITIANI, L. 2016. Metabolic/Proteomic Signature Defines Two Glioblastoma Subtypes With Different Clinical Outcome. *Sci Rep,* 6**,** 21557.

MERCER, T. R., DINGER, M. E. & MATTICK, J. S. 2009. Long non-coding RNAs: insights into functions. *Nat Rev Genet,* 10**,** 155-9.

MIZOGUCHI, M., GUAN, Y., YOSHIMOTO, K., HATA, N., AMANO, T., NAKAMIZO, A. & SASAKI, T. 2012. MicroRNAs in Human Malignant Gliomas. *J Oncol,* 2012**,** 732874.

MIZOGUCHI, M., GUAN, Y., YOSHIMOTO, K., HATA, N., AMANO, T., NAKAMIZO, A. & SASAKI, T. 2013. Clinical implications of microRNAs in human glioblastoma. *Front Oncol,* 3**,** 19.

MOLLINARI, C., RICCI-VITIANI, L., PIERI, M., LUCANTONI, C., RINALDI, A. M., RACANIELLO, M., DE MARIA, R., ZONA, C., PALLINI, R., MERLO, D. & GARACI, E. 2009. Downregulation of thymosin beta4 in neural progenitor grafts promotes spinal cord regeneration. *J Cell Sci,* 122**,** 4195-207.

MOOTHA, V. K., LINDGREN, C. M., ERIKSSON, K. F., SUBRAMANIAN, A., SIHAG, S., LEHAR, J., PUIGSERVER, P., CARLSSON, E., RIDDERSTRALE, M., LAURILA, E., HOUSTIS, N., DALY, M. J., PATTERSON, N., MESIROV, J. P., GOLUB, T. R., TAMAYO, P., SPIEGELMAN, B., LANDER, E. S., HIRSCHHORN, J. N., ALTSHULER, D. & GROOP, L. C. 2003. PGC-1alpha-responsive genes involved in oxidative phosphorylation are coordinately downregulated in human diabetes. *Nat Genet,* 34**,** 267-73.

OSTROM, Q. T., BAUCHET, L., DAVIS, F. G., DELTOUR, I., FISHER, J. L., LANGER, C. E., PEKMEZCI, M., SCHWARTZBAUM, J. A., TURNER, M. C., WALSH, K. M., WRENSCH, M. R. & BARNHOLTZ-SLOAN, J. S. 2014. The epidemiology of glioma in adults: a "state of the science" review. *Neuro Oncol,* 16**,** 896-913.

OSTROM, Q. T., COTE, D. J., ASCHA, M., KRUCHKO, C. & BARNHOLTZ-SLOAN, J. S. 2018a. Adult Glioma Incidence and Survival by Race or Ethnicity in the United States From 2000 to 2014. *JAMA Oncol,* 4**,** 1254-1262.

OSTROM, Q. T., GITTLEMAN, H., TRUITT, G., BOSCIA, A., KRUCHKO, C. & BARNHOLTZ-SLOAN, J. S. 2018b. CBTRUS Statistical Report: Primary Brain and Other Central Nervous System Tumors Diagnosed in the United States in 2011-2015. *Neuro Oncol,* 20**,** iv1-iv86.

OU, A., YUNG, W. A. & MAJD, N. 2020. Molecular mechanisms of treatment resistance in glioblastoma. *International journal of molecular sciences,* 22**,** 351.

PENG, Z., WU, T., LI, Y., XU, Z., ZHANG, S., LIU, B., CHEN, Q. & TIAN, D. 2016. MicroRNA-370-3p inhibits human glioma cell proliferation and induces cell cycle arrest by directly targeting beta-catenin. *Brain Res,* 1644**,** 53-61.

POTTOO, F. H., JAVED, M. N., RAHMAN, J. U., ABU-IZNEID, T. & KHAN, F. A. Targeted delivery of miRNA based therapeuticals in the clinical management of Glioblastoma Multiforme. Seminars in cancer biology, 2021. Elsevier, 391-398.

RICCI-VITIANI, L., PEDINI, F., MOLLINARI, C., CONDORELLI, G., BONCI, D., BEZ, A., COLOMBO, A., PARATI, E., PESCHLE, C. & DE MARIA, R. 2004. Absence of caspase 8 and high expression of PED protect primitive neural cells from cell death. *J Exp Med,* 200**,** 1257-66.

ROBERTS, T. C., LANGER, R. & WOOD, M. J. J. N. R. D. D. 2020. Advances in oligonucleotide drug delivery. 19**,** 673-694.

ROBSON, S. C., SEVIGNY, J. & ZIMMERMANN, H. 2006. The E-NTPDase family of ectonucleotidases: Structure function relationships and pathophysiological significance. *Purinergic Signal,* 2**,** 409-30.

SANA, J., BUSEK, P., FADRUS, P., BESSE, A., RADOVA, L., VECERA, M., REGULI, S., STOLLINOVA SROMOVA, L., HILSER, M. & LIPINA, R. 2018. Identification of microRNAs differentially expressed in glioblastoma stem-like cells and their association with patient survival. *Scientific reports,* 8**,** 1-11.

SCHMITT, A. M. & CHANG, H. Y. 2016. Long Noncoding RNAs in Cancer Pathways. *Cancer Cell,* 29**,** 452-463.

SHAHAR, T., GRANIT, A., ZRIHAN, D., CANELLO, T., CHARBIT, H., EINSTEIN, O., ROZOVSKI, U., ELGAVISH, S., RAM, Z., SIEGAL, T. & LAVON, I. 2016. Expression level of miRNAs on chromosome 14q32.31 region correlates with tumor aggressiveness and survival of glioblastoma patients. *J Neurooncol,* 130**,** 413-422.

SHAN, G., TANG, T., XIA, Y. & QIAN, H. J. 2020. Long non-coding RNA NEAT1 promotes bladder progression through regulating miR-410 mediated HMGB1. *Biomed Pharmacother,* 121**,** 109248.

SHERGALIS, A., BANKHEAD, A., 3RD, LUESAKUL, U., MUANGSIN, N. & NEAMATI, N. 2018. Current Challenges and Opportunities in Treating Glioblastoma. *Pharmacol Rev,* 70**,** 412-445.

SHI, J., DONG, B., CAO, J., MAO, Y., GUAN, W., PENG, Y. & WANG, S. 2017. Long non-coding RNA in glioma: signaling pathways. *Oncotarget,* 8**,** 27582-27592.

SHI, L., CHEN, J., YANG, J., PAN, T., ZHANG, S. & WANG, Z. 2010. MiR-21 protected human glioblastoma U87MG cells from chemotherapeutic drug temozolomide induced apoptosis by decreasing Bax/Bcl-2 ratio and caspase-3 activity. *Brain Res,* 1352**,** 255-64.

SINGH, S. K., HAWKINS, C., CLARKE, I. D., SQUIRE, J. A., BAYANI, J., HIDE, T., HENKELMAN, R. M., CUSIMANO, M. D. & DIRKS, P. B. 2004. Identification of human brain tumour initiating cells. *Nature,* 432**,** 396-401.

SLACK, F. J. & CHINNAIYAN, A. M. 2019. The role of non-coding RNAs in oncology. *Cell,* 179**,** 1033-1055.

SUBRAMANIAN, A., TAMAYO, P., MOOTHA, V. K., MUKHERJEE, S., EBERT, B. L., GILLETTE, M. A., PAULOVICH, A., POMEROY, S. L., GOLUB, T. R., LANDER, E. S. & MESIROV, J. P. 2005. Gene set enrichment analysis: a knowledge-based approach for interpreting genome-wide expression profiles. *Proc Natl Acad Sci U S A,* 102**,** 15545-50.

SYNNESTVEDT, K., FURUTA, G. T., COMERFORD, K. M., LOUIS, N., KARHAUSEN, J., ELTZSCHIG, H. K., HANSEN, K. R., THOMPSON, L. F. & COLGAN, S. P. 2002. Ecto-5'-nucleotidase (CD73) regulation by hypoxia-inducible factor-1 mediates permeability changes in intestinal epithelia. *J Clin Invest,* 110**,** 993-1002.

SZOPA, W., BURLEY, T. A., KRAMER-MAREK, G. & KASPERA, W. 2017. Diagnostic and Therapeutic Biomarkers in Glioblastoma: Current Status and Future Perspectives. *Biomed Res Int,* 2017**,** 8013575.

TANAKA, S., LOUIS, D. N., CURRY, W. T., BATCHELOR, T. T. & DIETRICH, J. 2013. Diagnostic and therapeutic avenues for glioblastoma: no longer a dead end? *Nat Rev Clin Oncol,* 10**,** 14-26.

UJIFUKU, K., MITSUTAKE, N., TAKAKURA, S., MATSUSE, M., SAENKO, V., SUZUKI, K., HAYASHI, K., MATSUO, T., KAMADA, K., NAGATA, I. & YAMASHITA, S. 2010. miR-195, miR-455-3p and miR-10a(*) are implicated in acquired temozolomide resistance in glioblastoma multiforme cells. *Cancer Lett,* 296**,** 241-8.

VERHAAK, R. G., HOADLEY, K. A., PURDOM, E., WANG, V., QI, Y., WILKERSON, M. D., MILLER, C. R., DING, L., GOLUB, T., MESIROV, J. P., ALEXE, G., LAWRENCE, M., O'KELLY, M., TAMAYO, P., WEIR, B. A., GABRIEL, S., WINCKLER, W., GUPTA, S., JAKKULA, L., FEILER, H. S., HODGSON, J. G.,

JAMES, C. D., SARKARIA, J. N., BRENNAN, C., KAHN, A., SPELLMAN, P. T., WILSON, R. K., SPEED, T. P., GRAY, J. W., MEYERSON, M., GETZ, G., PEROU, C. M., HAYES, D. N. & CANCER GENOME ATLAS RESEARCH, N. 2010. Integrated genomic analysis identifies clinically relevant subtypes of glioblastoma characterized by abnormalities in PDGFRA, IDH1, EGFR, and NF1. *Cancer Cell,* 17**,** 98-110.

WANG, J. & MATOSEVIC, S. 2019. NT5E/CD73 as correlative factor of patient survival and natural killer cell infiltration in glioblastoma. *Journal of clinical medicine,* 8**,** 1526.

WANG, W.-T., HAN, C., SUN, Y.-M., CHEN, T.-Q., CHEN, Y.-Q. J. J. O. H. & ONCOLOGY 2019. Noncoding RNAs in cancer therapy resistance and targeted drug development. 12**,** 1-15.

WIRSCHING, H. G., GALANIS, E. & WELLER, M. 2016. Glioblastoma. *Handb Clin Neurol,* 134**,** 381-97.

WOODS, B. J. & VAN VACTOR, D. 2021. miRNA: local guardians of presynaptic function in plasticity and disease. *RNA biology,* 18**,** 1014-1024.

WU, Z., SUN, H., ZENG, W., HE, J. & MAO, X. 2012. Upregulation of MircoRNA-370 induces proliferation in human prostate cancer cells by downregulating the transcription factor FOXO1. *PLoS One,* 7**,** e45825.

XU, W. P., YI, M., LI, Q. Q., ZHOU, W. P., CONG, W. M., YANG, Y., NING, B. F., YIN, C., HUANG, Z. W., WANG, J., QIAN, H., JIANG, C. F., CHEN, Y. X., XIA, C. Y., WANG, H. Y., ZHANG, X. & XIE, W. F. 2013. Perturbation of MicroRNA-370/Lin-28 homolog A/nuclear factor kappa B regulatory circuit contributes to the development of hepatocellular carcinoma. *Hepatology,* 58**,** 1977-91.

YAN, H. & BU, P. 2021. Non-coding RNA in cancer. *Essays in Biochemistry,* 65**,** 625-639.

YAN, Y., XU, Z., LI, Z., SUN, L. & GONG, Z. 2017. An Insight into the Increasing Role of LncRNAs in the Pathogenesis of Gliomas. *Front Mol Neurosci,* 10**,** 53.

ZENG, T., LI, L., ZHOU, Y. & GAO, L. 2018. Exploring Long Noncoding RNAs in Glioblastoma: Regulatory Mechanisms and Clinical Potentials. *Int J Genomics,* 2018**,** 2895958.

ZHA, L., ZHANG, J., TANG, W., ZHANG, N., HE, M., GUO, Y. & WANG, Z. 2013. HMGA2 elicits EMT by activating the Wnt/beta-catenin pathway in gastric cancer. *Dig Dis Sci,* 58**,** 724-33.

ZHANG, G., LAN, Y., XIE, A., SHI, J., ZHAO, H., XU, L., ZHU, S., LUO, T., ZHAO, T., XIAO, Y. & LI, X. 2019a. Comprehensive analysis of long noncoding RNA (lncRNA)-chromatin interactions reveals lncRNA functions dependent on binding diverse regulatory elements. *J Biol Chem,* 294**,** 15613-15622.

ZHANG, M., WU, W. B., WANG, Z. W. & WANG, X. H. 2017. lncRNA NEAT1 is closely related with progression of breast cancer via promoting proliferation and EMT. *Eur Rev Med Pharmacol Sci,* 21**,** 1020-1026.

ZHANG, P., WU, W., CHEN, Q. & CHEN, M. 2019b. Non-coding RNAs and their integrated networks. *Journal of integrative bioinformatics,* 16.

ZHANG, X., SUN, S., PU, J. K., TSANG, A. C., LEE, D., MAN, V. O., LUI, W. M., WONG, S. T. & LEUNG, G. K. 2012a. Long non-coding RNA expression profiles predict clinical phenotypes in glioma. *Neurobiol Dis,* 48**,** 1-8.

ZHANG, X., ZENG, J., ZHOU, M., LI, B., ZHANG, Y., HUANG, T., WANG, L., JIA, J. & CHEN, C. 2012b. The tumor suppressive role of miRNA-370 by targeting FoxM1 in acute myeloid leukemia. *Mol Cancer,* 11**,** 56.

ZHEN, L., YUN-HUI, L., HONG-YU, D., JUN, M. & YI-LONG, Y. 2016. Long noncoding RNA NEAT1 promotes glioma pathogenesis by regulating miR-449b-5p/c-Met axis. *Tumour Biol,* 37**,** 673-83.

ZIMMERMANN, H., ZEBISCH, M. & STRATER, N. 2012. Cellular function and molecular structure of ecto-nucleotidases. *Purinergic Signal,* 8**,** 437-502.

SUPPLEMENTARY FIGURES AND TABLES

Clinical features	Data
Median Age (range)	57 (42-72)
M/F	21/6
Localization	
Parietal	7
Frontal	11
Occipital	2
Temporal	7
Median Karnofsky performance (range)	75 (40-90)
Survival median (range)	12.2 (2-42)
MGMT status (M/UM)	13/14

Table 1. Clinical and pathological features of Glioblastoma patients.

Entrez Gene Id	Gene Symbol		HALLMARK EPITHELIAL MESENCHYMAL TRANSITION	HALLMARK TNFA SIGNALING VIA NFKB	HALLMARK UV RESPONSE DN	HALLMARK HEDGEHOG SIGNALING	HALLMARK HYPOXIA	HALLMARK IL2 STAT5 SIGNALING	HALLMARK INFLAMMATORY RESPONSE	HALLMARK INTERFERON GAMMA RESPONSE	HALLMARK KRAS SIGNALING UP	HALLMARK COAGULATION
7422	VEGFA											
7128	TNFAIP3											
56937	PMEPA1											
2669	GEM											
3486	IGFBP3											
4907	NT5E											
333	APLP1											
4323	MMP14											
5396	PRRX1											
4313	MMP2											
7057	THBS1											
5352	PLOD2											
7040	TGFB1											
51330	TNFRSF12A											
22795	NID2											
5744	PTHLH											
2152	F3											
2353	FOS											
2643	GCH1											
6347	CCL2											
7130	TNFAIP6											
2150	F2RL1											
8878	SQSTM1											
5606	MAP2K3											
1960	EGR3											

4929	**NR4A2**										
5271	**SERPINB8**										
57018	**CCNL1**										
7436	**VLDLR**										
8829	**NRP1**										
4233	**MET**										
3037	**HAS2**										
7035	**TFPI**										
5577	**PRKAR2B**										
23266	**ADGRL2**										
23345	**SYNE1**										
23576	**DDAH1**										
6334	**SCN8A**										
7048	**TGFBR2**										
1400	**CRMP1**										
154796	**AMOT**										
8828	**NRP2**										
10397	**NDRG1**										
5155	**PDGFB**										
6781	**STC1**										
54206	**ERRFI1**										
8406	**SRPX**										
284119	**CAVIN1**										
25819	**NOCT**										
55076	**TMEM45A**										
7133	**TNFRSF1B**										
4860	**PNP**										
115361	**GBP4**										
214	**ALCAM**										
990	**CDC6**										
4839	**NOP2**										
11230	**PRAF2**										
4135	**MAP6**										
5269	**SERPINB6**										
6335	**SCN9A**										

3091	**HIF1A**										
684	**BST2**										
6376	**CX3CL1**										
10630	**PDPN**										
8671	**SLC4A4**										
10437	**IFI30**										
51015	**ISOC1**										
196410	**METTL7B**										
25939	**SAMHD1**										
8869	**ST3GAL5**										
8404	**SPARCL1**										
23531	**MMD**										
23643	**LY96**										
26499	**PLEK2**										
3018	**HIST1H2BB**										
5801	**PTPRR**										
2934	**GSN**										
2	**A2M**										
11098	**PRSS23**										
1515	**CTSV**										
4485	**MST1**										

Table 2: Overlap of modulated genes in GSC#1 cells with restored expression of miR-370-3p. Hallmark gene sets with GSEA are shown**.**